

C.P. No. 307
(18,351)

A.R.C. Technical Report

C.P. No. 307
(18,351)

A.R.C. Technical Report



MINISTRY OF SUPPLY

**AERONAUTICAL RESEARCH COUNCIL
CURRENT PAPERS**

Turbulent Diffuser Flow

By

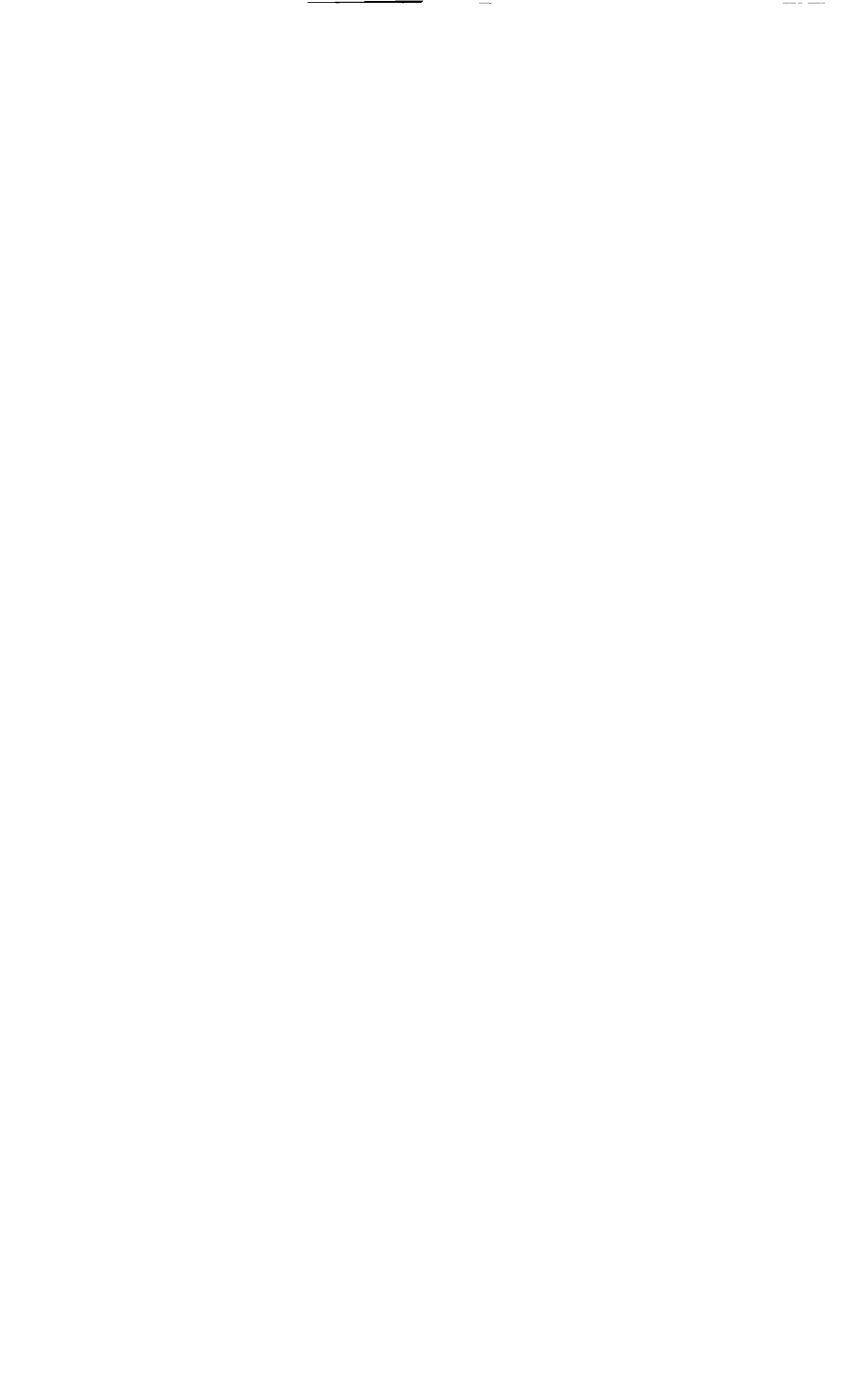
B. S. Stratford

**LIBRARY
ROYAL AIRCRAFT ESTABLISHMENT
BEDFORD.**

LONDON : HER MAJESTY'S STATIONERY OFFICE

1956

Price 7s 6d net



NATIONAL GAS TURBINE ESTABLISHMENT

Turbulent diffuser flow

- by -

E. S. Stratford

SUMMARY

Exact solutions of the equations of motion are possible for various types of diffuser. Application is restricted to that part of each diffuser in which the velocity profile has attained a constant shape. The solutions are expressed in terms of the distribution of the mixing length, which effectively is the length of the mean free path of the turbulence.

In particular the solutions yield the value of the critical angle of a diffuser for just avoiding flow separation; this value is proportional to the square of the turbulence level. If on the other hand the critical angle is known, use of the solutions in reverse allows an accurate assessment of the turbulence level. Thus if for the circular cone diffuser the critical total angle is 10° the turbulence estimated would be 30 per cent greater than that existing in the flow through a parallel pipe.

A detail of the solutions is that, if the mixing length close to the wall increases linearly with y the distance from the wall, the velocity profile in the separation condition approaches the form $u_r \propto y^{\frac{1}{2}}$.

Even in a flow which is diffusing rapidly a narrow wake becomes attenuated by the turbulence it produces. A large central wake, as from the bullet of a fan or turbine, is attenuated if the flow is of moderate diffusion angle. However the solutions suggest that a central wake, especially if produced by a high turbulence grid, could be used to advantage - for preventing flow separation in diffusers of very large angle.

If side jets are used for flow control at large diffuser angles and if the jets are required to persist a long distance downstream the jet velocity at any axial station would need to exceed twice the mean velocity for the cross-section.

CONTENTS

	<u>Page</u>
Preface	4
1.0 Introduction	4
2.0 The full form for the stresses in turbulent flow	5
2.1 Derivation using the full form for the stresses	7
3.0 The two-dimensional and axi-symmetric cone diffusers and free two-dimensional flow	12
3.1 A special "exact" solution	24
3.2 Free turbulence in two-dimensional flow	25
3.2.1 (i) The value of $\left(\frac{I_2}{b}\right)$;	27
(ii) the stability of the periodic velocity profile.	27
3.2.2 The behaviour of an isolated wake in diffusing flow	28
4.0 Wide angle two-dimensional diffusers with side jets or central wakes	28
4.1 Two-dimensional diffusers with side jets to prevent flow separation	29
4.1.1 The central core of flow $\delta_2 < y < 1.0$	29
4.1.2 The part of the profile between the jet peak and the velocity minimum	30
4.1.3 The jet "boundary layer" region, $0 < y < \delta_1$	34
4.1.4 The stability of the jet	36
4.1.5 The power expended in the jet	36
4.2 Two-dimensional diffusers of wind tunnels powered by injection; diffusers with central wakes - stabilised diffusers	37
5.0 Discussion	38
5.1 The absolute level of turbulence and its net rate of decay	38
5.2 The magnitude of the errors involved in using the sampler form for the turbulent stresses	40
5.3 Similarity with viscous and turbulent stresses	42
5.4 Some limitations on the flow	43
5.4.1 The pressure gradient and the root mean square velocity	43
5.4.2 Types of velocity profile	45

CONTENTS (Cont'd.)

	<u>Page</u>
6.0 Conclusions	47
List of Symbols	49
References	52

APPENDIX

<u>No.</u>	<u>Title</u>	
I	A tentative estimate of the effect of linearisation on the results for two-dimensional radial flow with free turbulence	54

ILLUSTRATIONS

<u>Fig. No.</u>	<u>Title</u>
1	The stresses on a small wedge of fluid
2	Various mixing length distributions
3	Various velocity profiles for the axi-symmetric diffuser at separation
4	Various velocity profiles for the two-dimensional diffuser at separation
5	Types of velocity profiles for diffusers with side jets or central wakes
6	The solution for the "boundary layer" of the jet
7	Types of velocity profiles in free two-dimensional radial flow - diffusing flow and accelerating flow
8	Types of velocity profiles in free two-dimensional radial flow - mixed diffusing and accelerating flow
9	The cubic equation for free two-dimensional radial flow

PREFACE

Much of the work reported in this paper was carried out in the Aeronautics Department of Imperial College.

1.0 Introduction

In the past little attention has been paid to the theoretical aerodynamics of the fully turbulent flow in diffusers, partly because simple empirical data - concerning for example the 6° cone - has proved adequate in many practical applications. A fuller understanding of the flow, however, might lead to suggestions for satisfying more exacting requirements. One theoretical investigation has been made by Gourzhienko¹ but, being restricted to flows of moderate diffusion rates, this investigation did not approach the condition of separation or stalling of the diffuser. The present paper obtains exact solutions of the equations of motion for flow which everywhere is just at the condition of separation. Application is limited to that part of a diffuser in which the velocity profile has reached a constant shape.

Standard mixing length theory² as developed mostly by Prandtl is the basis of the solutions. The philosophy of this theory is to explain the time-mean flow pattern by means of the mixing length distribution for the turbulence. The mixing length is not fundamental but it does have a physical interpretation, viz. the mean free path of the turbulent motion, and thereby it can contribute to an understanding of the flow. Accurate prediction is possible when the value of the mixing length is known, and for parallel flows in pipes and ducts this value has been well established, a single distribution holding universally provided the Reynolds number exceeds a certain minimum; for diffusing flows however no standard data is available and the subject is still controversial. Dönch³ and Nikuradse⁴ concluded from analyses of diffuser experiments that diffusion greatly increased the mixing length, but, in contrast, Ludwig and Tillmann⁵ found no such effect for a boundary layer when the pressure gradients were moderate. On the other hand Squire⁶ shows that, prior to the establishment of a steady profile shape in a conical diffuser, the change of profile is such as to suggest an increasing turbulence level, the final level probably exceeding that of flow in a pipe. As pointed out by Squire this qualitative result seems reasonable. If the turbulence is represented non-dimensionally by the ratio of the eddy velocity to the local mainstream velocity, diffusion will decrease the latter while not initially affecting the former; thus the ratio increases until, as will be examined in the present paper, a new equilibrium is established. The policy adopted in the present paper is therefore to use the little information which is available for the circular cone diffuser in order to re-estimate the effect of diffusion on the turbulence level, and then to apply the results to the assessment of other configurations.

One detailed point from the solutions is that in the velocity profile the gradient at the wall is infinite even at the separation condition, the profile asymptoting to the form $u_r \propto y^2$. This profile shape is in contrast to that for the corresponding laminar flow, where the gradient is zero and the asymptotic form is $u \propto y^3$, but it does nevertheless reflect experimental experience of turbulent flow under these conditions. Despite viscosity having been neglected the profile is realistic in being able to have a zero velocity at the wall.

The initial derivation uses a generalised form of the turbulent stress but the standard simpler form is adopted in the main analysis. Using either

form the equations for the time-mean motion reduce to a simple differential equation which in principle is readily solved.

2.0 The full form for the stresses in turbulent flow

The formula for shear stress conventionally used in mixing length theory on the basis of the momentum transfer hypothesis² is

$$\tau = \rho L^2 \left(\frac{\partial u}{\partial Y} \right) \left| \frac{\partial u}{\partial Y} \right| \dots\dots\dots(1a)$$

which, for positive values of $\frac{\partial u}{\partial Y}$, becomes

$$\tau = \rho L^2 \left(\frac{\partial u}{\partial Y} \right)^2 \dots\dots\dots(1b)$$

where $\left(\frac{\partial u}{\partial Y} \right)$ is the transverse gradient of velocity, ρ the density, and L a length related to the mean free path of the turbulent motion. It is also assumed conventionally that the normal pressure forces at a point are independent of direction, i.e.

$$P_{XX} = P_{YY} = -p \dots\dots\dots(2)$$

The above two relations are used for all the main calculations of the present paper, but it may be seen from a consideration of Figure 1 that strictly they are not internally consistent after transformation of axes. The stresses at a point if transplanted to act on a finite wedge of fluid would have to be in equilibrium; otherwise (following the standard proof used for showing that the pressure in an inviscid fluid is the same in all directions) for an infinitesimal wedge of fluid the ratio of resultant force to wedge mass would be proportional to

$$\frac{P_{XX}(\delta x)}{\rho(\delta x)^3}$$

and hence the fluid acceleration would tend to infinity as the wedge size approached zero.

For incompressible flow one system which would be internally consistent as regards transformation of axes is:

$$\begin{aligned}
 p_{XX} &= -p + \rho L^2 J e_{XX} \\
 p_{YY} &= -p + \rho L^2 J e_{YY} \\
 p_{XY} &= p_{YX} = \rho L^2 J e_{XY}
 \end{aligned}
 \tag{3a}$$

where J, an invariant in transformation, is

$$\begin{aligned}
 J &= \left| \left(\frac{1}{2}e_{XX}^2 + e_{XY}^2 + \frac{1}{2}e_{YY}^2 \right)^{\frac{1}{2}} \right| \\
 &= \left| \left(e_{XX}^2 + e_{YY}^2 \right)^{\frac{1}{2}} \right|
 \end{aligned}
 \tag{3b}$$

In these equations $e_{XX} (= -e_{YY})$ is equal to the difference of the rates of tensile strain and e_{XY} is the sum of the rates of shear strain, i.e.,

$$\begin{aligned}
 e_{XX} &= 2 \frac{\partial u_X}{\partial X} = \frac{\partial u_X}{\partial X} - \frac{\partial u_Y}{\partial Y} \\
 e_{YY} &= 2 \frac{\partial u_Y}{\partial Y} = \frac{\partial u_Y}{\partial Y} - \frac{\partial u_X}{\partial X} = -e_{XX} \\
 e_{XY} &= e_{YX} = \frac{\partial u_X}{\partial Y} + \frac{\partial u_Y}{\partial X}
 \end{aligned}
 \tag{3c}$$

$$\left(\frac{\partial u_X}{\partial X} = - \frac{\partial u_Y}{\partial Y} \text{ for an incompressible fluid} \right)$$

Equation (3) is a generalised form of Equation (1) and represents a consistent system for the turbulent or 'Reynolds stresses' provided only that the length L is taken as independent of the direction of the axes. This generalisation has been put forward by Prandtl and is quoted in Reference 7; it seems almost certainly to be a closer representation of real flow than is the conventional form represented by Equations (1) and (2). However the conventional form is much simpler and for flows with high shear, that is where $|e_{XY}| \gg |e_{XX}|$, the numerical difference is small. Consequently in the present paper whereas the full form is used in deriving the initial equations in order to show that the resultant flow still has similar velocity profiles, thereafter only the simpler form is used, a subsequent

check being made in order to estimate the magnitude of the effects caused by the simplification. The main derivation using the simpler form starts, almost from the beginning again, in Section 3.0.

2.1 Derivation using the full form for the stresses

The equations of motion for 'steady' turbulent two-dimensional incompressible flow may be written in terms of the Reynolds stresses and the local time-mean velocities as

$$\left. \begin{aligned} \frac{Du_X}{Dt} &= u_X \frac{\partial u_X}{\partial X} + u_Y \frac{\partial u_X}{\partial Y} = \frac{1}{\rho} \frac{\partial p_{XX}}{\partial X} + \frac{1}{\rho} \frac{\partial p_{YX}}{\partial Y} \\ \frac{Du_Y}{Dt} &= u_X \frac{\partial u_Y}{\partial X} + u_Y \frac{\partial u_Y}{\partial Y} = \frac{1}{\rho} \frac{\partial p_{YY}}{\partial Y} + \frac{1}{\rho} \frac{\partial p_{XY}}{\partial X} \end{aligned} \right\} \dots \dots \dots (4)$$

while the equation of continuity is

$$\frac{\partial u_X}{\partial X} + \frac{\partial u_Y}{\partial Y} = 0 \dots \dots \dots (5)$$

On transformation to cylindrical polar co-ordinates these equations become

$$\left. \begin{aligned} u_r \frac{\partial u_r}{\partial r} + \frac{u_\phi}{r} \frac{\partial u_r}{\partial \phi} - \frac{u_\phi^2}{r} &= \frac{1}{\rho r} \frac{\partial (r \cdot p_{rr})}{\partial r} + \frac{1}{\rho r} \frac{\partial p_{\phi r}}{\partial \phi} - \frac{1}{\rho r} p_{\phi\phi} \\ u_r \frac{\partial u_\phi}{\partial r} + \frac{u_\phi}{r} \frac{\partial u_\phi}{\partial \phi} + \frac{u_r u_\phi}{r} &= \frac{1}{\rho r} \frac{\partial p_{r\phi}}{\partial \phi} + \frac{1}{\rho r} \frac{\partial (r \cdot p_{r\phi})}{\partial r} + \frac{1}{\rho r} p_{\phi r} \end{aligned} \right\} \dots (6)$$

and

$$\frac{\partial (r \cdot u_r)}{\partial r} + \frac{\partial u_\phi}{\partial \phi} = 0 \dots \dots \dots (7)$$

Consideration is limited to pure radial flow; thus the whirl velocity is zero, i.e.

$$u_{\phi} = 0 \quad \dots\dots\dots(8)$$

Equations (7) and (8) give

$$\frac{\partial(r.u_r)}{\partial r} = 0$$

and therefore $(r.u_r)$ is a function of ϕ only, given by say

$$u_r = \frac{g(\phi)}{r} \quad \dots\dots\dots(9)$$

An example of such a flow would be flow with similar velocity profiles in a two-dimensional diffuser.

With Equations (8) and (9) Equations (6) reduce to

$$\left. \begin{aligned} u_r \frac{\partial u_r}{\partial r} &= \frac{1}{\rho r} \frac{\partial(r.p_{rr})}{\partial r} + \frac{1}{\rho r} \frac{\partial p_{\phi r}}{\partial \phi} - \frac{1}{\rho r} p_{\phi\phi} \quad \dots\dots(a) \\ 0 &= \frac{\partial p_{\phi\phi}}{\partial \phi} + \frac{\partial(r.p_{r\phi})}{\partial r} + p_{\phi r} \quad \dots\dots(b) \end{aligned} \right\} \dots\dots\dots(10)$$

Equation (3) giving the full form of the turbulent stress transforms in full to

$$\left. \begin{aligned} p_{rr} &= -p + \rho L^2 e_{rr}^J \\ p_{\phi\phi} &= -p + \rho L^2 e_{\phi\phi}^J \\ p_{r\phi} &= p_{\phi r} = \rho L^2 e_{\phi r}^J \end{aligned} \right\} \dots\dots\dots(11a)$$

with

$$\begin{aligned}
 J &= \left| \left(\frac{1}{2} e_{rr}^2 + e_{r\phi}^2 + \frac{1}{2} e_{\phi\phi}^2 \right)^{\frac{1}{2}} \right| \\
 &= \left| \left(e_{rr}^2 + e_{r\phi}^2 \right)^{\frac{1}{2}} \right|
 \end{aligned}
 \quad \left. \begin{array}{l} \\ \\ \end{array} \right\} \dots\dots\dots(11b)$$

and

$$\begin{aligned}
 e_{rr} &= 2 \frac{\partial u_r}{\partial r} = \frac{\partial u_r}{\partial r} - \left(\frac{1}{r} \frac{\partial u_\phi}{\partial \phi} + \frac{u_r}{r} \right) \\
 e_{\phi\phi} &= \frac{2}{r} \frac{\partial u_\phi}{\partial \phi} + \frac{2u_r}{r} = \left(\frac{1}{r} \frac{\partial u_\phi}{\partial \phi} + \frac{u_r}{r} \right) - \frac{\partial u_r}{\partial r} \\
 e_{r\phi} &= \frac{1}{r} \frac{\partial u_r}{\partial \phi} + \frac{\partial u_\phi}{\partial r} - \frac{u_\phi}{r}
 \end{aligned}
 \quad \left. \begin{array}{l} \\ \\ \\ \end{array} \right\} \dots\dots\dots(11c)$$

For flow in parallel pipes or ducts it is an accepted relation that the mixing length L is proportional to the duct width or diameter⁸. Thus in radial flow the mixing length may be expected to be proportional to the local width or diameter of the flow, and therefore proportional to the radius measured from the apex or 'source' of the flow. Hence it may be expressed

$$L = r \cdot \xi(\phi) \quad \dots\dots\dots(12)$$

Equations (11c) with Equations (8), (9) and (12) become

$$e_{rr} = 2 \frac{\partial u_r}{\partial r} = -\frac{2g}{r^2}$$

$$e_{\phi\phi} = \frac{2u_r}{r} = \frac{2g}{r^2}$$

$$e_{r\phi} = e_{\phi r} = \frac{1}{r} \frac{\partial u_r}{\partial \phi} = \frac{g'}{r^2}$$

thus, from (11b),

$$J = \frac{1}{r^2} | (4g^2 + g'^2)^{\frac{1}{2}} |$$

and finally, from (11a),

$$P_{rr} = -p - \frac{2\rho\xi^2 g}{r^2} | (4g^2 + g'^2)^{\frac{1}{2}} | \dots\dots\dots (13a)$$

$$P_{\phi\phi} = -p + \frac{2\rho\xi^2 g}{r^2} | (4g^2 + g'^2)^{\frac{1}{2}} | \dots\dots\dots (13b)$$

$$P_{r\phi} = P_{\phi r} = \frac{\rho\xi^2 g'}{r^2} | (4g^2 + g'^2)^{\frac{1}{2}} | \dots\dots\dots (13c)$$

With Equation (13c), Equation (10b) simplifies to

$$\frac{\partial P_{\phi\phi}}{\partial \phi} = 0 \dots\dots\dots (14)$$

which integrates to

$$P_{\phi\phi} = P_{\phi\phi}(r) \dots\dots\dots (15)$$

i.e. $P_{\phi\phi}$ is a function of r independent of ϕ .

Similarly Equation (10a) reduces to

$$\frac{\partial p}{\partial r} = \frac{\rho}{r^2} \left[\frac{\partial}{\partial \phi} \left(\xi^2 g' | (4g^2 + g'^2)^{\frac{1}{2}} | \right) + g^2 \right] \dots\dots\dots (16)$$

which integrates to

$$(P_{\infty} - p) = \frac{\rho}{2r^2} \left[\frac{\partial}{\partial \phi} \left(\xi^2 g' | (4g^2 + g'^2)^{\frac{1}{2}} | \right) + g^2 \right] \dots\dots\dots (17)$$

where P_∞ is the limiting static pressure as r tends to infinity. Equation (15b) shows that

$$P_\infty = -p_{\phi\phi, \infty} \dots\dots\dots(18)$$

Therefore, from Equation (15), P_∞ is a constant, independent of ϕ . Now Equations (17) and (15b) give

$$\frac{2r^2}{\rho} (P_\infty + p_{\phi\phi}) = \left[\frac{\partial}{\partial \phi} \left(\xi^2 g' \left| (4g^2 + g'^2)^{\frac{1}{2}} \right| \right) + g^2 - 4 \xi^2 \xi \left| (4g^2 + g'^2)^{\frac{1}{2}} \right| \right] \dots\dots\dots(19)$$

In this equation the left hand side is independent of ϕ and the right hand side is independent of r . Hence both sides must be equal to a constant, say B^2 .

Equating the left hand side to B^2 ,

$$p_{\phi\phi} = - \left[P_\infty - \frac{\rho B^2}{2r^2} \right] \dots\dots\dots(20)$$

and therefore, from Equation (15b),

$$p = P_\infty - \frac{\rho B^2}{2r^2} + \frac{2\rho \xi^2 \xi}{r^2} \left| (4g^2 + g'^2)^{\frac{1}{2}} \right| \dots\dots\dots(21)$$

Equating the right hand side to B^2 ,

$$\frac{d}{d\phi} \left(\xi^2 g' \left| (4g^2 + g'^2)^{\frac{1}{2}} \right| \right) + g^2 - 4 \xi^2 \xi \left| (4g^2 + g'^2)^{\frac{1}{2}} \right| = B^2 \dots\dots\dots(22)$$

Equation (22) is a simple differential equation which, if the mixing length distribution as represented by ξ is known, may be integrated for any specific boundary conditions to give $g(\phi)$ and hence the velocity distribution. Substitution of the result into Equations (20) and (21) would yield the pressure distribution. Equation (21) shows that the form of the pressure distribution is

$$p = P_{\infty} - \frac{\rho}{2r^2} \cdot (\text{function of } \phi)$$

This completes in principle the solution for two-dimensional radial flow using the full turbulent stresses; axis-symmetric three-dimensional flow similarly yields a solution. The remainder of the paper will base its calculations on the simpler form for the turbulent stresses, although a check will be made on the errors that this involves.

3.0 The two-dimensional and axis-symmetric cone diffusers and free two-dimensional flow

For completeness the solutions will start again almost from the beginning.

In terms of cylindrical polar co-ordinates the simpler assumptions for the turbulent stresses in two-dimensional flow as quoted in Equations (1b) and (2) become

$$P_{r\phi} = P_{\phi r} = \tau = \rho L^2 \cdot \left(\frac{1}{r} \frac{\partial u_r}{\partial \phi} \right)^2 \dots\dots\dots(23)$$

and

$$P_{rr} = P_{\phi\phi} = -P \dots\dots\dots(24)$$

The equations of motion are

$$u_r \frac{\partial u_r}{\partial r} + \frac{u_{\phi}}{r} \frac{\partial u_r}{\partial \phi} - \frac{u_{\phi}^2}{r} = \frac{1}{\rho r} \frac{\partial(r \cdot p_{rr})}{\partial r} + \frac{1}{\rho r} \frac{\partial p_{\phi r}}{\partial \phi} - \frac{1}{\rho r} p_{\phi\phi}$$

$$u_r \frac{\partial u_{\phi}}{\partial r} + \frac{u_{\phi}}{r} \frac{\partial u_{\phi}}{\partial \phi} + \frac{u_r u_{\phi}}{r} = \frac{1}{\rho r} \frac{\partial p_{\phi\phi}}{\partial \phi} + \frac{1}{\rho r} \frac{\partial(r \cdot p_{r\phi})}{\partial r} + \frac{1}{\rho r} p_{\phi r} \dots\dots\dots(6)_{bis}$$

and the equation of continuity is

$$\frac{\partial(r \cdot u_r)}{\partial r} + \frac{\partial u_{\phi}}{\partial \phi} = 0 \dots\dots\dots(7)_{bis}$$

If all the streamlines are radial

$$u_{\phi} = 0 \quad \dots\dots\dots(8)_{bis}$$

so that Equations (7)_{bis} and (8)_{bis} give

$$\frac{\partial(r \cdot u_r)}{\partial r} = 0$$

This integrates to give that the product (r.u_r) is a function of φ only, given by say

$$u_r = \frac{g(\phi)}{r} \quad \dots\dots\dots(9)_{bis}$$

With Equations (24) and (8)_{bis} the Equations of motion (6)_{bis} reduce to

$$\left. \begin{aligned} u_r \frac{\partial u_r}{\partial r} &= -\frac{1}{\rho} \frac{\partial p}{\partial r} + \frac{1}{\rho r} \frac{\partial p}{\partial \phi} \frac{\partial r}{\partial \phi} \\ 0 &= -\frac{\partial p}{\partial \phi} + \frac{\partial(r \cdot p_r)}{\partial r} + p_{\phi r} \end{aligned} \right\} \dots\dots\dots(25)$$

For fully turbulent flow in a pipe or duct of diameter or width 2h it is known⁸ that, above a certain Reynolds number, the ratio $\frac{L}{h}$ is a specific function of $\frac{y'}{h}$ where y' is the distance from the wall. It will be assumed that the same is true of diffuser flow, y' becoming the distance as measured along an arc from the wall. The function will for convenience be written

$$\frac{L}{h} = K \cdot f \left(\frac{y'}{h} \right) = K \cdot f(y) \quad \dots\dots\dots(26)$$

where $K = \left(\frac{\partial L}{\partial y'} \right)_{y'=0}$

and where $y = \frac{y'}{h}$

If the diffuser semi-angle is α

$$\left. \begin{aligned} h &= r \alpha \\ \text{and } y &= \frac{y'}{h} = \frac{\phi - \phi_0}{c} \end{aligned} \right\} \dots\dots\dots(27)$$

Hence y and therefore $f(y)$ are functions of ϕ independent of r . Equations (26) and (27) give the mixing length L in the form:

$$\left. \begin{aligned} L &= r \alpha K f(y) \\ &= r \alpha K f \end{aligned} \right\} \dots\dots\dots(28)$$

With Equations (28), (25) and (9)_{bis} the shear stress becomes

$$p_{r\phi} = p_{\phi r} = \tau = \rho \frac{\alpha^3}{r^3} \frac{K^2}{r^2} \frac{f^2}{2} \frac{g'^2}{2} \dots\dots\dots(29)$$

Substituting Equation (29) the Equations of motion (25) further reduce to

$$\left. \begin{aligned} \frac{\partial}{\partial r} (p + \frac{1}{2}\rho u_r^2) &= \rho \frac{\alpha^3}{r^3} \frac{K^2}{r^2} \frac{\partial}{\partial \phi} (f^2 g'^2) \dots\dots\dots(a) \\ 0 &= -\frac{\partial p}{\partial \phi} \dots\dots\dots(b) \end{aligned} \right\} \dots\dots\dots(30)$$

Since $u_r \rightarrow 0$ as $r \rightarrow \infty$ (see Equation (9)_{bis}) Equation (30a) integrates to

$$(p + \frac{1}{2}\rho u_r^2 - P_\infty) = -\rho \frac{\alpha^3}{2} \frac{K^2}{r^3} \frac{\partial}{\partial \phi} (f^2 g'^2)$$

i.e. from Equation (9)_{bis}

$$\frac{2r^2}{\rho} \cdot (P_\infty - p) = g^2 + \alpha^2 K^2 \frac{\partial}{\partial \phi} (r^2 g'^2) \dots\dots\dots(31)$$

In Equation (31) the left hand side is independent of ϕ since Equation (30b) gives $\frac{\partial p}{\partial \phi} = 0$, while the right hand side is independent of r . Hence both sides must be equal to a constant, say g_0^2 . Thus

$$\left. \begin{aligned} P_\infty - p &= \frac{\rho g_0^2}{2r^2} && \dots\dots(a) \\ g^2 + \alpha^2 K^2 \frac{\partial}{\partial \phi} (r^2 g'^2) &= g_0^2 && \dots\dots(b) \end{aligned} \right\} \dots\dots(32)$$

Equation (32b) is a simple differential equation for the velocity profile, the latter being represented by $g(\phi)$, which is defined in Equation (9)_{bis} (preceding Equation (25)). The solving of this equation requires that the mixing length distribution $L = K h f$ shall be known. Equation (32a) gives the form of the pressure distribution. By analogy with Equation (9)_{bis} Equation (32a) may be written

$$p + \frac{1}{2}\rho U_0^2 = P_\infty \dots\dots\dots(33)$$

Equation (32b) is conveniently integrated as follows.

The variables are changed from ϕ to y , where, from Equation (27)

$$\frac{d\phi}{dy} = \alpha \dots\dots\dots(34)$$

and from g to q , where

$$q = g/g_0 \dots\dots\dots(35)$$

Using dashes to denote differentiation with respect to y , the equation becomes

$$\frac{d}{dy} (r^2 q'^2) = \frac{\alpha}{K^2} (1 - q^2) \dots\dots\dots(36)$$

[The left hand side of this equation has derived from the term $\frac{\partial \tau}{\partial y}$, while the right hand side represents $\frac{\partial}{\partial r} (p + \frac{1}{2}\rho u_r^2)$ - as $p = P_\infty - \frac{1}{2}\rho U_0^2$, and $\frac{\partial}{\partial r} (-U_0^2 + u_r^2)$ is proportional to $(U_0^2 - u_r^2)$, or to $(1 - \frac{u_r^2}{U_0^2})$, i.e. to $(1 - q^2)$].

Now the value of α which has greatest practical interest is that for which the flow is just at the point of separation, i.e. for which the friction at the wall is (everywhere) just zero. The boundary conditions for the integration are therefore taken as

$$\begin{array}{l} u_r = 0 \\ \text{and } \tau_0 = 0 \end{array} \left. \vphantom{\begin{array}{l} u_r = 0 \\ \text{and } \tau_0 = 0 \end{array}} \right\} \begin{array}{l} \text{at } y' = 0 \\ \text{and at } y' = 2h \end{array}$$

i.e.

$$\begin{array}{l} q = 0 \\ \text{and } r^2 q'^2 = 0 \end{array} \left. \vphantom{\begin{array}{l} q = 0 \\ \text{and } r^2 q'^2 = 0 \end{array}} \right\} \begin{array}{l} \text{at } y = 0 \\ \text{and at } y = 2 \end{array}$$

It is more convenient, however, to replace the conditions at $y' = 2h$ by the conditions for symmetry about the centre line $y' = h$. The boundary conditions then become

$$\begin{array}{l} q = 0 \\ r^2 q'^2 = 0 \\ r^2 q'^2 = 0 \end{array} \left. \vphantom{\begin{array}{l} q = 0 \\ r^2 q'^2 = 0 \\ r^2 q'^2 = 0 \end{array}} \right\} \begin{array}{l} \text{at } y = 0 \\ \text{at } y = 0 \\ \text{at } y = 1 \end{array} \dots\dots\dots(37)$$

Of these three boundary conditions two are required because the differential equation is of the second order, whilst the third is required because the value of α is initially unknown.

Integration of Equation (36) between $y = 0$ and $y = 1$ and substitution from Equations (37) of the two boundary conditions concerning shear stress will be seen to give the useful alternative condition:-

$$\int_0^1 (1 - q^2) dy = 0 \quad \dots\dots\dots(a)$$

$$\text{i.e.} \quad \int_0^1 q^2 dy = 1 \quad \dots\dots\dots(b)$$

(On the basis of the representation following Equation (36) Equation (38a) may be regarded as the overall momentum condition, this taking a particularly simple form when, as here, the skin friction is continuously zero. Also, since $q = \frac{u_r}{U_0}$, multiplication of Equation (38b) by U_0^2 shows that U_0 , originally defined by Equation (33), is the root mean square value for the velocity profile:-

$$U_0^2 = \int_0^1 u_r^2 dy \quad \dots\dots\dots(38c)$$

These relations are investigated further in the discussion of Section 5.4.)

Successive integration of Equation (36) and incorporation of the boundary conditions at $y = 0$, from Equation (37), gives

$$f^2 q'^2 = \frac{\alpha}{K^2} \left[y - \int_0^y q^2 dy \right]$$

$$q = \frac{\alpha^{1/2}}{K} \int_0^y \frac{\left[y - \int_0^y q^2 dy \right]^{1/2}}{f} dy \quad \dots\dots\dots(39)$$

It is required to solve Equation (39) using the (initially unknown) value of α such that the resultant solution for q satisfies Equation (38). A

rapidly convergent solution by successive approximation is obtained by putting

$$I = \frac{K}{a^2} q \quad \dots\dots\dots(40)$$

The value of a is given, from Equation (38b), by

$$\frac{K^2}{a} = \int_0^1 I^2 dy \quad \dots\dots\dots(41)$$

while I is given by

$$I = \int_0^y \frac{\left[y - \frac{a}{K^2} \int_0^y I^2 dy \right]^{\frac{1}{2}}}{f} dy \quad \dots\dots\dots(42)$$

The n^{th} approximation to I , from Equation (42), gives the n^{th} approximation to a , by substitution into Equation (41); these values substituted into the right hand side of Equation (42) gives the $(n + 1)^{\text{th}}$ approximation to I . A suitable first approximation to I is

$$I_1 = 2 y^{\frac{1}{2}} \quad \dots\dots\dots(43)$$

which is the value obtained by taking only the dominant terms for small y on the right hand side of Equation (42), i.e. by omitting the term

$$\frac{a}{K^2} \int_0^y I^2 dy$$

and replacing f by y (see Equation (26)).

The method just used for finding the first approximation demonstrates also that the asymptotic behaviour near the wall is

$$I \sim 2 y^{\frac{1}{2}} \quad \text{as } y \rightarrow 0 \quad \dots\dots\dots(44)$$

The integration for small values of y is therefore performed algebraically in order to avoid numerical work near this singularity at $y = 0$.

From Equation (44) and earlier equations the form of the velocity profile near the wall is given by

$$\frac{u_r}{U_0} \sim \frac{2\alpha^{\frac{1}{2}}}{K} y^{\frac{1}{2}} = \frac{2\alpha^{\frac{1}{2}}}{K} \left(\frac{y'}{h} \right)^{\frac{1}{2}} \dots \text{ as } y' \rightarrow 0 \dots \dots (45a)$$

Thus the velocity becomes asymptotically proportional to the square root of the distance y' from the wall. From Equation (45a) the dynamic head behaves linearly with distance from the wall:-

$$\frac{1}{2}\rho u_r^2 \sim \frac{4\alpha}{K^2} \left(\frac{1}{2}\rho U_0^2 \right) \left(\frac{y'}{h} \right) \dots \text{ as } y' \rightarrow 0 \dots \dots (45b)$$

This may be re-expressed as

$$\frac{1}{2}\rho u_r^2 \sim \frac{2}{K^2} \frac{dp}{dr} y' \dots \text{ as } y' \rightarrow 0 \dots \dots (45c)$$

This expression is the same as that obtained in Reference 9 for the turbulent sub-layer of a turbulent boundary layer at separation. Both flows satisfy the asymptotic law

$$\tau \sim y' \frac{dp}{dr} \dots \text{ as } y' \rightarrow 0 \dots \dots (45d)$$

Equation (45a) shows that the value of $\frac{\partial u_r}{\partial y}$ at the wall is infinite and not zero, despite the wall shear stress being zero. (In a configuration for which the flow does definitely separate from the wall and a part of it reverse, as opposed to there being continuously zero skin friction as for the present analysis, there would be a tendency for the value of $\frac{\partial u_r}{\partial y}$ to change discontinuously, from infinity positive to infinity negative. Associated with this there would be sudden changes in velocity across the separation position in the region close to the wall. Sudden changes such as these are a well known feature of turbulent flow separation. In practice the discontinuity would be softened by the presence of viscous stresses; in addition, as discussed in Reference 9, a new type of turbulence appears to be set up, after the conditions represented by Equation (45) have been reached - but prior to actual separation, and then a zero value for $\left(\frac{\partial u_r}{\partial y} \right)_{y=0}$ does seem possible.)

Before discussing further the results of the integration, the corresponding equations will be quoted for the axi-symmetric cone diffuser as there the value of α can readily be compared with experimental results.

Proceeding by the same method as for the two-dimensional diffuser the axi-symmetric diffuser yields the following equations.

Corresponding to Equation (32a):-

$$P_{\infty} - p = \frac{\rho g_0^2}{2r^4} \dots\dots\dots(46)$$

a repetition of Equation (33):-

$$p + \frac{1}{2}\rho U_0^2 = P_{\infty} \dots\dots\dots(47)$$

corresponding to Equation (36):-

$$\frac{d}{dy} \left[(1 - y) r^2 q'^2 \right] = \frac{2\alpha}{K^2} (1 - y) (1 - q^2) \dots\dots\dots(48)$$

corresponding to Equation (38):-

$$\int_0^1 (1 - y) (1 - q^2) dy = 0$$

i.e.

$$\int_0^1 (1 - y) q^2 dy = \frac{1}{2}$$

}(49)

and, corresponding to Equation (39):-

$$q = \frac{2^{-\frac{1}{2}} \alpha^{\frac{1}{2}}}{K} \int_0^y \frac{\left[y \left(1 - \frac{y}{2}\right) - \int_0^y (1 - y) q^2 dy \right]^{\frac{1}{2}}}{f (1 - y)^{\frac{1}{2}}} dy \dots\dots\dots(50)$$

Equation (50) is readily solved by putting

$$I = \frac{K}{2^{2\frac{1}{3}} c^{\frac{1}{3}}} u \quad \dots\dots\dots(51)$$

so that α is given by

$$\frac{K^2}{4\alpha} = \int_0^1 (1-y) I^3 dy \quad \dots\dots\dots(52)$$

while I is given by

$$I = \int_0^y \frac{\left[y \left(1 - \frac{y}{2}\right) - \frac{2c}{K^2} \int_0^y (1-y) I^3 dy \right]^{\frac{1}{2}}}{f (1-y)^{\frac{1}{2}}} dy \quad \dots\dots\dots(53)$$

A suitable first approximation is again

$$I_1 = 2 y^{\frac{1}{2}}$$

and the procedure of successive approximation follows as before.

The asymptotic behaviour of I near the wall is still

$$I \sim 2 y^{\frac{1}{2}} \quad \dots\dots \quad \text{as } y \rightarrow 0$$

Thus the asymptotic form of the velocity profile near the wall satisfies

$$\frac{u_r}{U_0} \sim \frac{2 \alpha^{\frac{1}{2}} 2^{\frac{1}{2}}}{K} y^{\frac{1}{2}} = \frac{2 \alpha^{\frac{1}{2}} 2^{\frac{1}{2}}}{K} \left(\frac{y'}{h} \right)^{\frac{1}{2}}$$

$$\frac{1}{2} \rho u_r^2 \sim \frac{8\alpha}{K^2} \left(\frac{1}{2} \rho U_0^2 \right) \left(\frac{y'}{h} \right)$$

as $y' \rightarrow 0$

or
$$\frac{1}{2} \rho u_r^2 \sim \frac{2}{K^2} \frac{dp}{dr} y'$$

..... (54)

and
$$\tau \sim y' \frac{dp}{dr}$$

The above constitutes a method whereby the limiting cone angle and the velocity profile for the separation condition of the flow may be calculated for any given mixing length distribution. Alternatively the solution may be used in reverse so that if the limiting value of the diffuser angle is known the level of the turbulence could be calculated. (This procedure would have a good accuracy since in the theory the turbulence level varies according to only the square root of the limiting cone angle - for example Equation (48) shows that $K \propto \alpha^2$.)

The first calculation is made for the circular cone assuming that the mixing length distribution is the same as that characteristic of parallel flow in pipes. This distribution⁶, denoted L_0 , and shown in Figure 2 as curve (a), gives successive values of $\frac{\alpha}{K^2}$ (in the algebraic process of successive approximation developed above) to be 0.575, 0.328, 0.3195 and 0.3175, so that the end value may be taken as 0.317. With $K = 0.408$ as for parallel flow this gives $\alpha = 3.04^\circ$ so that the total cone angle 2α is 6.08° . The velocity profile is shown in Figure 3 as curve (a).

For comparison the calculation was repeated using the mixing length distribution suggested by Dönch³ and Nikuradse⁴ after analyses of experiments on two-dimensional diffusers. The distribution has been denoted $L_{D.N.}$ and is shown in Figure 2 as curve (b). It yields a total angle of 15.5° for the circular cone at separation. The corresponding velocity profile is shown in Figure 3 as curve (b).

Now while in practice the total angle suitable for providing a stable flow not over-sensitive to inlet conditions is found to be 6° , the limiting angle for just avoiding flow separation is known to be at least 10° , as shown in Reference 6. Since the limiting angle α is proportional to K^2 , comparison of the experimental 10° result, with the 6.08° result obtained above, indicates that the turbulence level for flow in the 10° circular cone must be at least 50 per cent higher than for parallel flow, but perhaps not so high as the level suggested by Dönch and Nikuradse⁴. It would seem that this increase in

¹Although the distribution of Dönch and Nikuradse was obtained from experiment it is not fully conclusive as, in addition to requiring the differentiation of an experimental velocity profile, their analysis involves a small difference of large quantities. The difference is particularly small near the wall where the mixing length is most important, and the accuracy of the large quantities may be affected by the non-two-dimensionality in the flow resulting from the 'end wall' boundary layer.

turbulence level over that of parallel flow can be explained as follows.

In the fully developed parallel flow the absolute value of the turbulence as represented by $(\overline{u'_x u'_y})^2$ remains constant, its level being determined by the equilibrium between the production and the decay of the turbulence. In the fully developed diffuser flow $(\overline{u'_r u'_\theta})^2$ must decrease in proportion to the mainstream speed, represented by say U_0 , in order that $\frac{(\overline{u'_r u'_\theta})^2}{U_0}$ shall remain constant and the whole flow display simi-

arity. Thus the rate of decay must exceed the rate of production of turbulence. This disturbing of the previous balance requires the new steady state to be established at a higher level, as then the higher turbulence would give an increased decay rate and hence the required excess of decay over production. Comparison of flow at one particular cross-section of a diffuser with a parallel flow of the same mean velocity as at that cross-section should therefore show the diffuser to have the higher turbulence*.

As corollaries to the preceding argument it is to be expected firstly that all diffusing flows would have a somewhat higher turbulence than parallel flow - because the balance between decay and production has been disturbed - and secondly that the more rapid the diffusion the greater the increase in the turbulence level. These corollaries are needed when assessing the calculations in the remainder of the paper since, in most instances, use is made of the known mixing length distribution for parallel flow. The practical conclusion is conveniently simple. It will have been noticed that the limiting angle predicted for the circular cone when using this distribution characteristic of parallel flow was equal to the value found suitable in practice for providing satisfactorily stable diffusion. This correlation - between the theoretical prediction and the practical requirement - should hold in general for those types of diffuser where the diffusion rate is about equal to that for the circular cone. On the other hand for configurations achieving very rapid diffusion the prediction would be expected to represent only a lower limit to the true practical possibilities.

As may have been seen from the Figures the shape of the velocity profile predicted on the basis of L_0 is correct in its general form but it probably is not very accurate as regards detail (the actual experimental profile is not known); for example $L_{D,N}$ is better in showing the straight middle portion usually found in experimental profiles for turbulent flows near separation. Thus diffusing flow, besides having a higher general level of turbulence compared with parallel flow, has also a somewhat modified shape for its turbulence distribution.

Figure 2 curve (c) represents an additional example for the circular cone diffuser illustrating the influence of the assumption concerning mixing length. The distribution shown by the curve would lead to a limiting cone angle of 6° and a velocity profile almost the same as given by $L_{D,N}$.

*This does not mean that when fully developed pipe flow enters a diffuser the absolute value of the turbulence - say $(\overline{u'_r u'_\theta})^2$ - increases; the non-dimensional value $\frac{(\overline{u'_r u'_\theta})^2}{U_0}$ would increase initially due to the

decrease in U_0 , as pointed out in Reference 6, and it is presumably in this way that the new steady state would be reached.

Returning now to the two-dimensional diffuser the distribution L_0 leads to $\alpha = 3.99^\circ$ giving therefore a limiting total angle of 8° ; the velocity profile is shown in Figure 4 as curve (a). The value for the total angle obtained experimentally by Nikuradse¹⁰ was between 9.6° and 10.2° . Exact comparison with experiment would be prevented by effects from the end wall boundary layers, unless special precautions were taken in the experiment.

3.1 A special "exact" solution

In the method used so far the equations of motion have been shown to transform and reduce exactly to a simple differential equation, but this equation has had to be integrated numerically. Were the mixing length distribution a disposable function it would be possible to find exact solutions to the differential equation - merely by postulating the velocity distribution in some algebraic form and substituting to find the mixing length required to satisfy the equation. It so happens that one of these mixing length distributions is quite a reasonable approximation to the actual practical one and has a particularly simple form; it is such as to give the velocity exactly proportional to the square root of the distance from the wall. This 'special' distribution, denoted L_s , is given by

$$\begin{array}{l}
 L_s = K y' \left(1 - \frac{y'}{h}\right)^{\frac{1}{2}} \\
 \text{i.e. } L_s = K h y (1 - y)^{\frac{1}{2}} \\
 \text{and } f = y (1 - y)^{\frac{1}{2}}
 \end{array}
 \left.
 \begin{array}{l}
 \\
 \\
 \\
 \end{array}
 \right\} \dots\dots\dots(55)$$

It is shown in Figure 2 as curve (d). The solutions to the differential equations are as follows.

For the two-dimensional diffuser

$$\begin{array}{l}
 \frac{u_r}{U_0} (= q) = (2 y)^{\frac{1}{2}} = \left(\frac{2 y'}{h}\right)^{\frac{1}{2}} \\
 \text{and } \frac{\alpha}{K^2} = \frac{1}{2}
 \end{array}
 \left.
 \begin{array}{l}
 \\
 \\
 \end{array}
 \right\} \dots\dots\dots(56)$$

Using $K = 0.408$ the diffuser total angle becomes $2 \alpha = 9.5^\circ$, (as compared with 8.0° obtained from the mixing length distribution for parallel flow).

For the axi-symmetric cone diffuser

$$\frac{u_r}{U_0} (= q) = (3 y)^{\frac{1}{2}} = \left(\frac{3 y'}{h} \right)^{\frac{1}{2}} \dots\dots\dots (57)$$

and $\frac{\alpha}{K^2} = \frac{3}{8}$

Using $K = 0.408$ the diffuser total angle is $2 \alpha = 7.15^\circ$, compared with 6.0° for the parallel flow distribution.

The velocity distributions are shown in Figure 4 as curve (b) and in Figure 3 as curve (c).

The main error in the form of this mixing length distribution is at the centre of the diffuser; this region is not important in determining the limiting diffuser angle as the stress there falls to zero. The results are therefore useful when some simple analytical representation is required for the flow, and might be considered analogous to the standard power law approximations for the turbulent boundary layer on a flat plate.

3.2 Free turbulence in two-dimensional flow

Consideration is now given to a two-dimensional purely radial flow in which the velocity is an oscillatory function of the angular position ϕ , as for example in Figure 7a. There are no wall boundaries present to require a zero velocity or to restrict the turbulence and consequently it will be referred to as 'free-two-dimensional flow'. The corresponding standard parallel flow is that sometimes called "the turbulent wake behind a row of parallel rods"¹¹. As in the standard theory the mixing length is assumed proportional to the wavelength of the velocity distribution but independent of the position on the waveform.

The equations of motion are identical with those for the two-dimensional diffuser and only the boundary conditions and the mixing length are changed. The differential equation for the velocity profile, corresponding to Equation (36) for the two-dimensional diffuser, is

$$\frac{d}{dy} (q'^2) = \frac{\lambda}{2c^2} (1 - q^2) \dots\dots\dots (58)$$

where now $y = \frac{y'}{b}$

$2b =$ the linear wavelength of the velocity profile

and $c = \frac{L}{b}$.

The boundary conditions are

$$\begin{array}{l}
 \frac{\partial u}{\partial \phi} = 0 \left\{ \begin{array}{l} \text{when } \phi = 0 \\ \text{and} \\ \text{when } \phi = \frac{\lambda}{2} \end{array} \right\} \\
 \text{i.e.} \quad \frac{dq}{dy} = 0 \left\{ \begin{array}{l} \text{when } y = 0 \\ \text{and} \\ \text{when } y = 1 \end{array} \right\}
 \end{array} \quad \dots\dots\dots(59)$$

The equation could be integrated direct (numerically) but for simplicity it is linearised. It then becomes similar to the linearised equation for the standard parallel flow. Putting

$$q = (1 + t) \quad \dots\dots\dots(60)$$

with the maximum value of t equal to t_M , integration of the linearised equation gives that the angular wavelength λ is

$$\begin{array}{l}
 \lambda = 23.1 t_M c^2 \\
 \text{or} \quad \lambda = 23.1 t_M \left(\frac{L}{b} \right)^2
 \end{array} \quad \dots\dots\dots(61)$$

Details of the mathematics of the linearised solution and of the corresponding velocity profile are as for the standard flow¹¹.

A tentative comparison between the results from the linearised equation and those which would be obtained from the full equation is given in Appendix I. This comparison suggests that when the value of t_M is say 20 per cent, none of the effects of linearisation exceed about 3 per cent, while if suitable mean values are used (e.g. if in Equation (61) the mean of t_{max} and $(-t)_{max}$ is used in place of t_{max} .) the effect on λ is less than 1 per cent when t_M is 20 per cent.

The next Section 3.2.1, which considers the stability of the periodic velocity profile, will consider also the value to be expected in practice for $\left(\frac{L}{b} \right)$, and will mention an example on this type of flow.

The result just obtained for turbulent flow may be compared with that for free two-dimensional laminar flow, which gives, for the velocity profile:-

$$\frac{t}{t_M} = \sin \left(\left[\frac{2 r U_0}{v} \right]^{\frac{1}{2}} \cdot \phi \right)$$

and therefore, for the wavelength:-

$$\lambda = \frac{2 \Pi}{\left[\frac{2 r U_0}{v} \right]^{\frac{1}{2}}}, (r U_0 = \text{const.} = \xi_0)$$

.....(62)

3.2.1 (i) The value of $\left(\frac{L}{b} \right)$;

(11) the stability of the periodic velocity profile

(1) The above analysis shows that a diffusing flow is possible having a constant percentage velocity variation, of magnitude proportional to the angular wavelength of the flow profile. From Equation (61) the amplitude $\pm t_M$ is

$$t_M = \frac{\lambda}{23.1 \left(\frac{L}{b} \right)^2}$$

For the corresponding parallel flow Schlichting found the value of $\frac{L}{b}$ to be $\frac{L}{b} = 0.293$. (Reference 2 but p.169). On the other hand a somewhat similar factor obtained for jet mixing at Göttingen has a value 0.096. (Reference 2 but p.173). For the jet mixing the flow geometry differs from that for the wakes and a lower value of the factor would be expected. Hence for wake mixing it is probably conservative to assume say that $\frac{L}{b} = 0.20$. (The value in practice would be expected to depend somewhat on the total number of wakes as eventually the wake flow will be bounded by a low turbulence mainstream or a solid boundary). Thus using say $\frac{L}{b} = 0.20$, t_M becomes

$$t_M = 1.08 \lambda$$

If λ is to be expressed in degrees, it is convenient to write the final result as

$$t_M = 0.019 \lambda \cdot (\text{degrees}^{-1}) \quad \text{.....(63)}$$

(11) Whereas the analysis so far gives the solution for the flow in which the velocity profile remains similar at all cross sections, a flow for which the initial value of t_M differed from that given by Equation (63) could not maintain a constant t_M and it might be questioned whether t_M

would tend towards the steady value or diverge from it. By considering the forces on say a half wavelength width of fluid for which $u_r < U_0$ and by supposing that t_M exceeds the value from Equation (63), but that otherwise the profile shape is similar to that for similar solutions, it is readily shown that the value of t_M will tend towards the steady value. In this sense, therefore, the flow is stable. It seems likely that the flow is stable more generally, so that any two-dimensional radial flow in which the velocity is a periodic function of the angular position will adjust itself until the velocity variation satisfies Equation (63) (or the corresponding equation using the actual values of $\frac{L}{b}$).

Example

A two-dimensional diffuser has boundary layer control in order to allow the use of a 40° total angle. It is required to find the behaviour of the main flow when this contains wakes of a wavelength equal to a tenth of the diffuser width.

The value of λ is $\frac{40^\circ}{10} = 4^\circ$

From Equation (63) the steady value for t_M , $= \frac{u_r - U_0}{U_0}$, is

$$t_M = 0.019 \times 4 = 8 \text{ per cent}$$

On the argument given above the flow profile is 'stable', hence the velocity variation would tend to ± 8 per cent of the local cross section mean velocity.

3.2.2 The behaviour of an isolated wake in diffusing flow

In the diffuser of a wind tunnel only a single wake is likely to be present. This single wake will tend to spread across the flow at the same time as it adjusts itself to a certain value for t_M . Eventually, if the diffuser were very long, and the wake losses large compared with the losses at the wall, the wake would spread across the diffuser and the flow would become similar to that illustrated in Figure 5b. This flow will be discussed in Section 4.2. For the early flow, however, while the wake is still remote from the walls, it seems probable that the arguments developed above for the periodic velocity profile would roughly apply. The example just given therefore shows that even if a wind tunnel employed very rapid diffusion a narrow wake should still become attenuated by the turbulence it produces, provided it were not sufficiently close to a solid boundary for this turbulence to be impeded.

4.0 Wide angle two-dimensional diffusers with side jets or central wakes

Two types of wide angle diffuser with side jets will be examined, that when the side jets are intended only to prevent separation of the flow from the wall, and that in a wind tunnel which is powered by injection.

The two types of profile are illustrated in Figures 5a and 5b respectively. A diffuser with a central wake would have the type of profile shown in Figure 5b. Such a flow would occur downstream of the 'bullet' of a fan or turbine, and downstream of a bluff model in a wind tunnel working section. As will be suggested later it could also be made to occur intentionally, in order to stabilise the flow in a wide angle diffuser. Practical applications would be likely to have axi-symmetric flow but for simplicity the theory will be only for two-dimensional diffusers.

Pure radial flow is again assumed, so that the velocity profiles are similar at all radii.

4.1 Two-dimensional diffusers with side jets to prevent flow separation

Let the co-ordinates of the velocity profile satisfy the various parameters shown in Figure 5a, i.e. the values of $q \left(= \frac{u}{U_0} \right)$ are: $q = q_1$ at the jet peak, which is at a distance $y = \frac{y'}{h} = \delta_1$ from the wall, and $q = q_2$ at $y = \delta_2$, which is where the velocity is a minimum. The three parts of the velocity profile separated by the lines $y = \delta_1$ and $y = \delta_2$ will each be treated individually.

The diffuser angle may be related to the parameters quoted above and the stability and power of the jet examined.

4.1.1 The central core of flow $\delta_2 \leq y \leq 1.0$

This portion of the flow is remote from the walls and the mixing length will be almost constant across it. Thus the free turbulence theory of the previous Section 3.2 may be applied provided a suitable value is chosen for the mixing length L. The result of the linearised theory of Section 3.2 is

$$\lambda = 25.1 t_M \left(\frac{L}{b} \right)^2 \dots\dots\dots (61)_{PLS}$$

and the maximum values of t and $(-t)$ from the linear theory are equal. Hence

$$t_M = -t_{u1} = (1 - q_2) \dots\dots\dots (61)$$

Also, from the geometry of the flow

"Figure 5a would result only if the main velocity profile had "deteriorated" before the flow reached the injection position. If the injection air were applied before deterioration of the profile, i.e. when the profile consisted of a constant velocity mainstream and thin boundary layers, then considerations of boundary layer control would be more appropriate, rather as considered, for example, in References 12, 13 and 14.

$$\lambda = 2 \cdot (1 - \delta_2)$$

and

$$b = (1 - \delta_2) h$$

}(65)

Thus Equation (61) becomes

$$2 \alpha (1 - \delta_2) = \frac{25.1 (1 - q_2)}{(1 - \delta_2)^3} \left(\frac{L}{h} \right)^2$$

i.e.

$$\alpha = \frac{11.55 (1 - q_2)}{(1 - \delta_2)^3} \left(\frac{L}{h} \right)^2 \quad \dots\dots\dots(66)$$

The diffuser angle is therefore determined given δ_2 and q_2 only, for a given value of the mixing length.

Example

Suppose $q_2 = 0.6$; $\delta_2 = 0.45$

The mixing length distribution for parallel flow shown in Figure 2 curve (a) suggests a value for $\frac{L}{h}$ of 0.12. Equation (66) then gives

$$\alpha = \frac{(11.55)(0.4)}{(0.55)^3} (0.12)^2 = 0.359 \text{ rad}$$

The comparison of Appendix I which estimates the effect of linearisation suggests that the value of α if calculated without linearisation would be within a few per cent of:-

$$\alpha = 0.354 \text{ rad, } = 20.3^\circ; \text{ i.e. } 2 \alpha = 40.6^\circ$$

This is to be compared with the value of 8° for the simple two-dimensional diffuser of Section 3.0. A proportion of the 40.6° is occupied by the flow from the control jet. The proportion so occupied is estimated later to be just over 5 per cent.

4.1.2 The part of the profile between the jet peak and the velocity minimum

This region is defined by $\delta_1 \leq y \leq \delta_2$. Relations are required in order to determine δ_1 and q_1 given δ_2 and q_2 .

Since in this region of the flow the velocity gradient $\frac{\partial u}{\partial y}$ is negative the basic equation for shear stress

$$\tau = \rho L^2 \left(\frac{\partial u}{\partial Y} \right) \left| \frac{\partial u}{\partial Y} \right| \dots\dots\dots (1a)_{bis}$$

now becomes

$$\tau = - \rho L^2 \left(\frac{\partial u}{\partial Y} \right)^2, \text{ for } \left(\frac{\partial u}{\partial Y} \right) < 0 \dots\dots\dots (67)$$

The motion being two-dimensional and radial from the vertex the equations of motion must reduce to the simple differential equation of Section 3.0, except for a change of sign. Thus

$$\frac{d}{dy} (r^2 q'^2) = - \frac{a}{K^2} (1 - q^2) \dots\dots\dots (68)$$

where

$$q = \frac{u_r}{U_o}, y = \frac{y'}{h}$$

and the mixing length is

$$L = K h f; f = f (y)$$

In order to be able to obtain a result algebraically it is assumed that the mixing length is proportional to the distance from the wall. Then

$$\left. \begin{aligned} L &= K y' = K h y \\ \text{and} \quad f &= y \end{aligned} \right\} \dots\dots\dots (69)$$

For convenience the variable y is replaced by η given by

$$\eta = \frac{y}{\delta_2} \dots\dots\dots (70)$$

and then Equation (68) reduces to

$$\frac{d}{d\eta} (\eta^2 q'^2) = -\frac{\alpha \delta_2^2}{K^2} (1 - q^2) \dots\dots\dots(71)$$

where q' now represents $\frac{dq}{d\eta}$. Since $\frac{dq}{d\eta}$ is zero at $\eta = \frac{\delta_1}{\delta_2}$ and at $\eta = 1$ integration of Equation (71) gives that the overall condition to be satisfied is:-

$$\int_{\frac{\delta_1}{\delta_2}}^1 (1 - q^2) d\eta = 0 \dots\dots\dots(72)$$

The solution to (71) may be found reasonably conveniently as follows:-
Let γ be the root of the associated equation

$$\frac{d}{d\eta} (\eta^2 \gamma'^2) = -\frac{\alpha \delta_2^2}{K^2} (1 - q_2^2) \dots\dots\dots(73)$$

where the variable term q^2 on the right hand side of Equation (71) has been replaced by q_2^2 , the value at $\eta = 1$. Successive integration between the limits η and 1 (these limits are chosen as Equation (73) will not permit $\frac{d\gamma}{d\eta}$ being zero at $\eta = \frac{\delta_1}{\delta_2}$, if a real solution is postulated between $\eta = \frac{\delta_1}{\delta_2}$ and $\eta = 1$ having $\frac{d\gamma}{d\eta} = 0$ at $\eta = 1$) gives

$$\gamma = q_2 + \left[\frac{\alpha \delta_2^2}{K^2} (1 - q_2^2) \right]^{\frac{1}{2}} \int_{\eta}^1 \frac{(1 - \eta)^{\frac{1}{2}}}{\eta} d\eta \dots\dots\dots(74)$$

i.e.

$$\gamma = q_2 + \left[\frac{\alpha \delta_2^2}{K^2} (1 - q_2^2) \right]^{\frac{1}{2}} \left[2 \operatorname{sech}^{-1} \eta^{\frac{1}{2}} - 2 (1 - \eta)^{\frac{1}{2}} \right] \dots\dots\dots(75)$$

or, putting $q_3^2 = (1 - q_2^2)$ (76)

$$\gamma = q_2 + 2q_3 \left(\frac{\alpha \delta_2^2}{K^2} \right)^{\frac{1}{2}} \left[\operatorname{sech}^{-1} \eta^{\frac{1}{2}} - (1 - \eta)^{\frac{1}{2}} \right] \dots\dots\dots(77)$$

It may then be shown that the original Equation (71) has an approximate solution:

$$q = \gamma + \varepsilon \dots\dots\dots(78a)$$

where $\varepsilon \doteq - (1 + q_2) \frac{\alpha \delta_2}{K^2} F(\eta) \dots\dots\dots(78b)$

and

$$F(\eta) = \int_{\eta}^1 \frac{\int_{\eta}^1 \left[\operatorname{sech}^{-1} \eta^{\frac{1}{2}} - (1 - \eta)^{\frac{1}{2}} \right] d\eta}{\eta (1 - \eta)^{\frac{1}{2}}} d\eta \dots\dots\dots(78c)$$

i.e.

$$F(\eta) = 2 \left[\frac{1}{3} \left\{ (1 - \eta) + 2 \log \frac{1}{\eta} \right\} - (1 - \eta)^{\frac{1}{2}} \operatorname{sech}^{-1} \eta^{\frac{1}{2}} \right] \dots\dots\dots(78d)$$

The differential of this solution is not sufficiently accurate for determining $\frac{\delta_1}{\delta_2}$, i.e. the value of η at which $\frac{dq}{d\eta} = 0$, but substitution of the Equation (78) into the integral condition (72) does provide adequate accuracy.

Having thus determined the value of $\eta = \frac{\delta_1}{\delta_2}$, the value of q_1 at this position is obtained, though not so accurately, by direct substitution into Equation (78).

Example

The example taken for the core of the flow is continued through this region. The data is:

$$K = 0.408 \quad ; \quad q_2 = 0.6$$

$$\delta_2 = 0.43 \quad ; \quad \frac{\alpha \delta_2}{K^2} = 0.910$$

Numerical integration of Equation (72), after substitution of the data into Equation (78), gives $\frac{\delta_1}{\delta_2} = 0.034$, i.e. $\delta_1 = 0.015$. Substitution of

$\eta = \frac{\delta_1}{\delta_2} = 0.034$ into Equation (78) gives $q_1 = 1.9$ (which value will not be as accurate as that for $\frac{\delta_1}{\delta_2}$).

As $\frac{\alpha \delta_2}{K^2}$ decreases, $\frac{\delta_1}{\delta_2}$ decreases to zero and q_1 increases to infinity. There is a minimum value of $\frac{\alpha \delta_2}{K^2}$ for which $\frac{\delta_1}{\delta_2}$ is real. By considering the value of $\int_0^1 (1 - \gamma^2) d\eta$ it may be shown that when $q_2 = 0.6$ this minimum value is certainly greater than 0.347 rad; for $K = 0.408$ the value of $(\alpha \delta_2)$ must therefore exceed 3.3° .

4.1.3 The jet "boundary layer" region of the profile,
 $0 < y < \delta_1$

The simple differential equation for the velocity profile is solved as in the previous section to give:

$$q = q_1 - 2q_2 \left(\frac{\alpha \delta_1}{K^2} \right)^{\frac{1}{2}} T \left(\frac{y}{\delta_1} \right) + 2q_1 \frac{\alpha \delta_1}{K^2} F \left(\frac{y}{\delta_1} \right) \dots\dots\dots(79)$$

where $q = q_1$ at $\frac{y}{\delta_1} = 1$,

$$q_2^2 = q_1^2 - 1 \dots\dots\dots(80a)$$

where $F \left(\frac{y}{\delta_1} \right)$ is the same function, but with $\left(\frac{y}{\delta_1} \right)$ in place of η , as in Equation (78d), and where $T \left(\frac{y}{\delta_1} \right)$ is the bracketed function in Equation (77):-

$$T \left(\frac{y}{\delta_1} \right) = \left[\operatorname{sech}^{-1} \left(\frac{y}{\delta_1} \right)^{\frac{1}{2}} - \left(1 - \frac{y}{\delta_1} \right)^{\frac{1}{2}} \right] \dots\dots\dots(80b)$$

If the wall skin friction is positive the velocity profile must asymptote at the wall to the semi-empirical form:

$$\frac{q}{q_\tau} = \frac{u}{u_\tau} \sim A + \frac{1}{K} \log \frac{y^+ u_\tau}{\nu} \dots\dots\dots(81)$$

It is found that this condition is satisfied provided the following relation holds between the velocity at the jet peak and the distance of the jet peak from the wall.

$$\frac{1 + 2 (1 - \log 2) \left(1 - \frac{1}{q_1^2}\right)^{\frac{1}{2}} \left(\frac{\alpha \delta_1}{K^2}\right)^{\frac{1}{2}} - 4 \left(\log 2 - \frac{1}{3}\right) \left(\frac{\alpha \delta_1}{K^2}\right)}{\left(1 - \frac{1}{q_1^2}\right)^{\frac{1}{2}} \left(\frac{\alpha \delta_1}{K^2}\right)^{\frac{1}{2}} - \frac{2}{3} \left(\frac{\alpha \delta_1}{K^2}\right)} =$$

$$AK + \log \left[\frac{K^3 R_0}{\alpha} q_1 \left(\frac{\alpha \delta_1}{K^2}\right) \left\{ \left(1 - \frac{1}{q_1^2}\right)^{\frac{1}{2}} \left(\frac{\alpha \delta_1}{K^2}\right)^{\frac{1}{2}} - \frac{2}{3} \frac{\alpha \delta_1}{K^2} \right\} \right] \dots\dots\dots (82)$$

where $R_0 = \frac{h U_0}{\nu} \dots\dots\dots (82a)$

Figure 6 expresses this relation as a series of curves of q_1 against $\frac{\alpha \delta_1}{K^2}$, for various values of R_0 (from 10^4 to 10^9), when α and K are given the values 20° and 0.408 respectively. Since α occurs only in the variable $\frac{\alpha \delta_1}{K^2}$ and in the parameter $\frac{K^3 R_0}{\alpha}$, solutions for other values of α may be obtained from the curves by factoring the value chosen for R_0 . The curves are not exact as graphical interpolation has been used in their derivation from Equation (82).

Example

Further continuing the previous example, the data is:

$$K = 0.408 \quad ; \quad \alpha = 20.3^\circ (\cong 20^\circ);$$

$$\delta_1 = 0.015 \quad ; \quad \frac{\alpha \delta_1}{K^2} = 0.031;$$

also the previous solution required $q_1 = 1.9$.

Figure 6 shows that $q_1 = 1.9$ and $\frac{\alpha \delta_1}{K^2} = 0.031$ are compatible provided the Reynolds number R_0 is 3×10^5 . For other Reynolds numbers these values would be incompatible and the profile across the whole section would have to adjust itself until a compatible system were obtained. Thus it is not possible to postulate entirely arbitrarily the initial values say of δ_2 and q_2 .

4.1.4 The stability of the jet

Supposing the jet suffers a slight disturbance such that its non-dimensional velocity q and its angular width (something greater than $\alpha \delta_1$) are affected, but its volume flow is unaffected. If it may be assumed that the volume flow is proportional to the product of q and δ_1 , then this product would remain sensibly constant. The jet may be considered as stable if, after the disturbance, it tends to return to its former angular width and non-dimensional velocity, and unstable if it continues to change in the same sense as the disturbance. In analysing the jet stability it is assumed permissible to neglect the change in pressure gradient that would result from the jet disturbance having affected the main flow. It may then be argued - at some length - that the jet will be stable only if the position of operation on the curve of q against $\frac{\alpha \delta_1}{K^2}$, for the appropriate Reynolds number, is above (in the sense of a larger value of q) the position where $\left(q \cdot \frac{\alpha \delta_1}{K^2} \right)$ is a minimum. The locus of points of minimum $q \cdot \frac{\alpha \delta_1}{K^2}$ is shown in Figure 6 as a broken line, this represents the stability limit. It will be seen that for stable operation the peak jet velocity must exceed approximately twice the velocity U_0 , where $p + \frac{1}{2}\rho U_0^2 = P_\infty$, almost independently of Reynolds number.

4.1.5 The power expended in the jet

For a uniform velocity jet the power expended in the injection is equal to the product of the jet velocity, the slot width, and the excess of the jet total head over the diffuser static pressure at infinity. If the velocity profile that has been calculated above the distance of the jet peak from the wall is equal to $h \delta_1$, but the full equivalent jet width is several times larger than this, as much of the flow between δ_1 and δ_2 would be injection air. Suppose that the equivalent jet width is say $n h \delta_1$, n being quite large when $\frac{\delta_1}{\delta_2}$ is as small as 0.034 as in the example calculated. The "power factor of injection", if this is defined as the ratio of the power expended on injection to the power regained in the diffuser main flow, (excluding injection air) then becomes;

$$\text{Power Factor} = \frac{q_1 (n \delta_1) (q_1^2 - 1)}{(1 - q n \delta_1)} \dots\dots\dots(83)$$

(In deriving this expression the total volume flow has been put equal to $2h U_0$.)

For the value $q_1 = 2.0$, the minimum value for stability,

and for $\delta_1 = 0.015$, as in the example calculated above,

Equation (83) gives

$$\text{Power Factor} = \frac{0.09 n}{(1 - 0.03 n)}$$

It is estimated that n is about four for this value of δ_1 . Thus the power expended on injection is about 40 per cent of the power regained in the main flow in that length of the diffuser between the position of injection and infinity.

In practical applications a wide angle diffuser is likely to be short, and it may not be necessary to maintain a stable jet. If desirable, the value of q_1 used for the jet velocity could probably be much less than the stability limit of 2.0, (although the jet width would then probably need to be larger than in the example calculated). Moreover, Equation (83) shows that the power expended is very sensitive to q_1 . For example the value of the product $q_1 (q_1^2 - 1)$ changes from 6.0 to 1.875 when q_1 changes from 2.0 to 1.5. It seems quite likely therefore that a power expenditure on injection more in the region of 20 per cent, rather than of 40 per cent, of the power regained in the main flow of the diffuser, would be sufficient for a short wide angle diffuser for which the velocity profile has already "deteriorated".

4.2 Two-dimensional diffusers of wind tunnels powered by injection; diffusers with central wakes - stabilised diffusers

For this type of diffuser the velocity profile is of the type shown in Figure 5b, with a maximum at $y = \delta$ and a minimum at the centre at $y = 1$.

Considering this very briefly, the central region defined by $\delta \leq y \leq 1$ may be treated by the free turbulence theory of Section 3.2, just as for the core of the flow in the previous section. Thus, following Equation (66),

$$\alpha = \frac{11.55 (1 - q_{min})}{(1 - \delta)^3} \left(\frac{L}{h} \right)^2 \dots\dots\dots(84)$$

The region between the wall and the jet peak could be treated accurately by the method of Section 3.0, for a given mixing length distribution, but for convenience it will be compared with a half of a simple two-dimensional diffuser. As the jet flow is close to the wall the mixing length L will be almost as great as the value $L = Ky$. Consequently the mixing length for a half of a simple diffuser will underestimate L , and it will therefore underestimate the limiting angle, between the wall and the velocity peak, at which the jet is in the separation condition. Since the simple diffuser semi-angle is 4° the jet will not separate if $(\alpha \delta) < 4^\circ$. (The "exact" solution of Section 3.1 would probably still underestimate the angle so that the jet should not separate if $(\alpha \delta) < 4.75^\circ$.)

The stability criterion of the previous section is not readily applied to this type of flow as changes in the jet would be likely to affect the pressure gradient significantly.

Example

For $\delta = 0.2$ and $q_{min} = \frac{2}{3}$

Figure 2 curve (a) suggests $\frac{L}{h} = 0.10$

Equation (84) gives $2\alpha = 8.6^\circ$ and $(\alpha \cdot \delta) = 0.86^\circ$

The above analysis applies also to diffusers having central wakes instead of side jets, as has been discussed in the first paragraph of Section 4.0. This type of profile would be obtained in a diffuser if the wake losses were comparable with the losses at the wall. An application of such a flow would be to the stabilising of a very wide angle diffuser by means of a gauze, or a turbulence grid, at entry - across only the central portion of the flow. The following example indicates that this should be more effective than a gauze across the whole cross section.

Example

In order to stabilise a diffuser in which space is more important than maximum efficiency a gauze, or grid, is placed across the central portion of the entry flow. The arrangement is such that the characteristics of the resulting profile are roughly equivalent to

$$\delta = 0.3, q_{\min} = \frac{1}{3}$$

Figure 2 curve (a) suggests $\left(\frac{L}{h}\right) = 0.11$. Equation (84) then gives that the total angle of the diffuser is $(2\alpha) = 31.2^\circ$. The diffusion is therefore about four times as rapid as for the simple two-dimensional diffuser.

Since $\delta = 0.3$ the value of $(\alpha \cdot \delta)$ is 4.7° ; the flow which passes between the gauze and the wall is thus approaching the separation condition.

Use of a simple central gauze would damp the turbulence below the value assumed above. On the other hand since the diffusion is very rapid the steady state turbulence level should be very high, as discussed in Section 3.0. Thus if a special high turbulence grid were used in order to convert main stream velocity in the central portion of the flow into high turbulence, the turbulence would be expected to persist at a high level and the consequent cone angle could be very large - significantly larger than predicted above - provided care could be taken at entry.

5.0 Discussion

The discussion is concerned with certain largely theoretical aspects of the subject.

5.1 The absolute level of turbulence and its net rate of decay

Since a knowledge of the mixing length amounts almost to a knowledge of the turbulence it is not surprising that the foregoing calculations allow estimation of the turbulence level in a diffuser. With the relation

$$\tau = -\rho \overline{u'_r u'_\phi} = \rho L^2 \left(\frac{\partial u'_r}{\partial y'_r} \right)^2 \dots\dots\dots (85)$$

the value of $\overline{u'_r u'_\phi}$ could be calculated directly by differentiating the velocity profile and substituting the value of the mixing length. Under some circumstances it would be more accurate however to integrate the equations of motion and obtain, for the two-dimensional diffuser,

$$\tau = -\rho \overline{u'_r u'_\phi} = \rho U_0^2 c \int_0^y (1 - q^2) dy \dots\dots\dots(86)$$

thus employing an integral of the velocity profile. Substitution of $q = (2y)^{1/2}$, as obtained in Section 3.1, is adequate for showing the main behaviour. This gives

$$-\overline{u'_r u'_\phi} = U_0^2 c y (1 - y) \dots\dots\dots(87)$$

so that the maximum value of $|\overline{u'_r u'_\phi}|$ across the section is at the position $y = \frac{1}{2}$, where

$$|\overline{u'_r u'_\phi}|_{\max.} = \frac{1}{4} U_0^2 c \dots\dots\dots(88)$$

or

$$|\overline{u'_r u'_\phi}|_{\max.}^{1/2} = \frac{U_0}{2} c^{1/2} \dots\dots\dots(89)$$

If, for example, 2α were 8° , as obtained in Section 3.0 when using the mixing length distribution for parallel flow, Equation (89) would give

$$|\overline{u'_r u'_\phi}|_{\max.}^{1/2} = 0.14 U_0 \dots\dots\dots(90)$$

For the axi-symmetric diffuser

$$-\overline{u'_r u'_\phi} = 2 U_0^2 c y (1 - y) \dots\dots\dots(91)$$

and for $2\alpha = 6^\circ$ as obtained in Section 3.0 (again with the parallel flow mixing length),

$$|\overline{u'_r u'_\phi}|_{\max.}^{1/2} = 0.16 U_0 \dots\dots\dots(92)$$

Thus for both diffusers the maximum value of $|\overline{u'_r u'_\phi}|^2$ at any section would be approximately 15 per cent of the root mean square velocity U_0 at that section. This would become 20 per cent if the actual critical angle

is 10° for the axi-symmetric diffuser, and say 14° for the two-dimensional diffuser.

As discussed earlier not only the absolute level of turbulence but also the net rate of decay may be calculated once the limiting cone angle is known. The difference from pipe flow is that in the latter the net rate of decay for any section as a whole is zero. From the derivation above, or merely by postulating similarity between the turbulent eddy velocities and the main radial velocity, the turbulence level decreases in proportion with the main radial velocity. Hence it decreases proportionally to $\frac{1}{r}$ for the two-dimensional diffuser and to $\frac{1}{r^2}$ for the axi-symmetric diffuser. Thus for any portion of the fluid prediction could be made for the net rate of decay of $u'r$ or $u'r^2$ either with respect to time or with respect to distance.

This net rate of decay affects the balance between the decay and the production of turbulence and hence influences the turbulence level in the steady state, as discussed in Section 5.0.

5.2 The magnitude of the errors involved in using the simpler form for the turbulent stresses

In using the simpler form for the turbulent or 'Reynolds stresses', i.e.,

$$\tau_{XY} = \rho L^2 \left| \frac{\partial u}{\partial Y} \right| \left(\frac{\partial u}{\partial Y} \right) \dots\dots\dots (1a)_{b1s}$$

and
$$p_{XX} = p_{YY} = -p \dots\dots\dots (2)_{b1s}$$

two changes have been made from the proposed more accurate form, which was as follows:-

$$\left. \begin{aligned} p_{XX} &= -p + \rho L^2 J e_{XX} \\ p_{YY} &= -p + \rho L^2 J e_{YY} \\ p_{XY} &= p_{YX} = \rho L^2 J e_{XY} \end{aligned} \right\} \dots\dots\dots (3a)_{b1s}$$

$$\left. \begin{aligned} J &= \left| \left(\frac{1}{2} e_{XX}^2 + e_{XY}^2 + \frac{1}{2} e_{YY}^2 \right)^{\frac{1}{2}} \right| \\ &= \left| \left(e_{XX}^2 + e_{XY}^2 \right)^{\frac{1}{2}} \right| \end{aligned} \right\} \dots\dots\dots (3b)_{b1s}$$

$$\begin{aligned}
 e_{XX} &= 2 \frac{\partial u_X}{\partial X} = \frac{\partial u_X}{\partial X} - \frac{\partial u_Y}{\partial Y} \\
 e_{YY} &= 2 \frac{\partial u_Y}{\partial Y} = \frac{\partial u_Y}{\partial Y} - \frac{\partial u_X}{\partial X} = -e_{XX} \\
 e_{XY} &= e_{YX} = \frac{\partial u_X}{\partial Y} + \frac{\partial u_Y}{\partial X}
 \end{aligned}
 \quad \dots\dots\dots (3c)_{b1s}$$

The change in the shear stress is to replace J by $\frac{\partial u}{\partial Y}$; the change in the normal stress is to omit the terms such as $\rho L^2 e_{XX} J$, thereby implying that the normal stresses are each equal to minus the static pressure. The simplifications amount to assuming that the rates of tensile strain $\frac{\partial u_X}{\partial X}$ and $\frac{\partial u_Y}{\partial Y}$, and the rate of cross shearing strain $\frac{\partial u_Y}{\partial X}$, are small compared with the longitudinal shearing strain $\frac{\partial u_X}{\partial Y}$.

Most turbulent flows have become turbulent because of the instability of a large shearing velocity in the lammar flows from which they derive. A large shearing velocity is still present after the transition has taken place so that generally turbulent flows are flows with high shear. Since the axes are conventionally chosen so that the high shear is represented by $\frac{\partial u_X}{\partial Y}$, (or $\frac{\partial u_r}{\partial \phi}$), this becomes the dominant term and the simplifications are reasonably justified. Some of the effects of the simplification will be investigated for the two-dimensional diffuser.

In the two-dimensional radial flows considered the static pressure predicted by the simpler theory has been constant at any given radius. The result using the more exact theory is that the normal stress $p_{\phi\phi}$ is constant, as given by Equation (14). On the latter theory the variation of static pressure across the section would be, (from Equation (11)),

$$\begin{aligned}
 \delta p &= -\delta p_{\phi\phi} + \delta (\rho L^2 e_{\phi\phi} J) \quad \dots\dots\dots (93) \\
 &= 0 + \delta (\rho L^2 e_{\phi\phi} J) \\
 &= \delta (\rho L^2 e_{\phi\phi} e_{r\phi})
 \end{aligned}$$

i.e.

$$\delta p = \delta \left(2 \rho L^2 \frac{u_r}{r^2} \frac{\partial u_r}{\partial \phi} \right) \quad \dots\dots\dots (94)$$

Making use of the special solution of Section 3.1 the maximum value of this static pressure variation is

$$\begin{aligned}
 (\delta p)_{\max.} & \doteq \frac{1}{2} \rho U_0^2 \cdot \frac{16 K^2 a}{27} \\
 & \doteq 0.007 \left(\frac{1}{2} \rho U_0^2 \right)
 \end{aligned}
 \quad \dots\dots\dots (95)$$

Thus, for the separation flow, the variation of static pressure across any section is given as zero by the approximate theory, but as just under 1 per cent of the section mean dynamic head by the more accurate theory.

Similarly the ratio of the shear stress, $p_{r\phi}$, of the more accurate theory, to the shear stress τ of the simpler theory, for a given value of the mixing length L , is

$$\frac{p_{r\phi}}{\tau} = \left[1 + \left(\frac{2r \frac{\partial u_r}{\partial r}}{\frac{\partial u_r}{\partial \phi}} \right)^2 \right]^{\frac{1}{2}} \quad \dots\dots\dots (96)$$

At the peaks of velocity this ratio locally tends to infinity. Whereas, using τ , the profile asymptotes to a $3/2$ power law at the peak, using $p_{r\phi}$ the asymptotic form is a square law (i.e. if (δu_r) and (δy) are the departures from the values at the peak, the profiles corresponding to the two assumptions satisfy respectively: $(\delta u_r) \propto (\delta y)^{3/2}$, and $(\delta u_r) \propto (\delta y)^2$). For free turbulence the mean value of $p_{r\phi}$ is about 10 per cent higher than that of τ . This could presumably be absorbed into the empirical value for the mixing length. In diffusers the difference is less than this 10 per cent.

5.3 Similarity with viscous and turbulent stresses

If in any flow the stresses are made up of both turbulent and viscous components then for it to be possible for the velocity profiles to be strictly similar at say all radial stations there must be "dimensional compatibility" between the turbulent and viscous components. In particular the ratio of the two components at any point on the profile must be the same at all radial stations, i.e., the ratio must be independent of the radius. The dimensions of the ratio of the turbulent to the viscous shear stress are given by:

$$\begin{aligned}
 \frac{\text{turbulent stress}}{\text{viscous stress}} & = \frac{\rho L^2 \left(\frac{\partial u_r}{\partial y^2} \right)^2}{\mu \left(\frac{\partial u_r}{\partial y^2} \right)} \\
 & = \frac{L^2}{\nu} \frac{\partial u_r}{\partial y^2}
 \end{aligned}$$

For radial flow with similarity

$$u_r = \frac{g(\phi)}{r^n}$$

where $n = 1$ for two-dimensional flow

and $n = 2$ for axi-symmetric flow.

Also

$$y' = r \phi, \text{ i.e. } \frac{\partial}{\partial y'} = \frac{1}{r} \frac{\partial}{\partial \phi}$$

and

$$L = K h f = K r a f$$

hence

$$\frac{\text{turbulent stress}}{\text{viscous stress}} = \left(\frac{K^2 a^2 f^2 g'}{\nu} \right) r^{1-n} \dots\dots\dots(97)$$

Thus the ratio is independent of the radius only if $n = 1$, i.e., only for the two-dimensional flow and not for the axi-symmetric flow. This difficulty has not appeared in the present paper as in the main analysis only turbulent stresses have been considered, a procedure which has been possible because the analysis has been restricted to flow at the separation condition. For that condition it happens that a realistic solution can be obtained independently of viscosity, even at the wall, because in the region where viscosity is usually important, i.e. in the viscous sub-layer close to the wall, the stress is either zero or very small.

For conditions other than with the flow just at separation the usual logarithmic behaviour would occur at the wall. Being a function of Reynolds number this would give similarity only for two-dimensional flow. It is possible as in Reference 1 to obtain approximate similarity in axi-symmetric flow if the Reynolds number variation is not excessive; the Reynolds number along the diffuser is inversely proportional to the radius.

The above suggests that the separation condition for the axi-symmetric cone is particularly suited to investigations into turbulent flow, quite apart from the practical interest associated with the limiting rate of flow diffusion. For flows other than at separation axi-symmetric flow does not have strict similarity and thus analysis is difficult; for two-dimensional flow the end wall boundary layers would either complicate the experiment or complicate comparison with theory.

5.4 Some limitations on the flow

5.4.1 The pressure gradient and the root mean square velocity

In the analysis of the preceding sections the velocity U_0 has been defined by the Bernoulli equation type of relationship:

$$p + \frac{1}{2}\rho U_0^2 = \text{const.} = P_\infty \quad \dots\dots\dots(33)_{bls}$$

It is found (Equation (38c)) that for flows at the separation condition U_0 becomes the section root mean square velocity.

Physically the above is because at the separation condition the skin friction and hence the externally applied shear force is zero, and so the momentum derivation of the Bernoulli equation, i.e.

$$dp = -\rho u \, du$$

must apply, not locally, but if the quantities are summed across the section:-

$$\int_A dp \, dA = - \int_A \rho u_r \, du_r \, dA \quad \dots\dots\dots(98)$$

where dA is an element of the sectional area A . Since the pressure is constant across the section

$$A \, dp = - \rho \int_A d(u_r^2) \, dA$$

Assuming that the order of operations may be inverted, (intuitively because there are similar profiles at all stations),

$$dp = - \frac{\rho}{A} d\left(\int_A u_r^2 \, dA\right)$$

On integration this becomes

$$p + \frac{1}{2} \rho \int_A u_r^2 \, \frac{dA}{A} = P_\infty \quad \dots\dots\dots(99)$$

Therefore, by comparing Equations (33)_{bls} and (99)

$$U_0^2 = \int_A u_r^2 \, \frac{dA}{A} \quad \dots\dots\dots(100)$$

In addition to being true of diffuser flow at separation this relation holds for the flow in any stream tube which represents a surface of zero shear stress. A further example is the flow between the positions of maximum and minimum velocity in the free two-dimensional flow of Section 3.2.

If the skin friction is not zero the final pressure rise is reduced and the value of U_0 as defined by

$$p + \frac{1}{2}\rho U_0^2 = \text{const.} = P_\infty \dots\dots\dots(33)_{\text{bis}}$$

would be less than the root mean square velocity across the section.

5.4.2 Types of velocity profile

Consideration is again given to the value $U = U_0$ defined by Equation (33):-

$$p + \frac{1}{2}\rho U_0^2 = \text{const.} = P_\infty \dots\dots\dots(33)_{\text{bis}}$$

and attention is still restricted to radial flows with similar velocity profiles at all radii. Most of the arguments are concerned with the 'free two-dimensional flow' of Section 3.2.

In diffusing flow the pressure rise that will occur between station r and infinity is equal to the value of $\frac{1}{2}\rho U_0^2$ at station r , from the above Equation (33), and in accelerating flow the pressure fall that has already taken place between infinity and station r is equal to $\frac{1}{2}\rho U_0^2$. Thus fluid which has zero net shear force acting upon it (i.e. where $\frac{\partial \tau}{\partial \phi}$ is locally zero) and which must therefore behave according to the Bernoulli equation, i.e. with constant total head, must have a velocity equal to U_0 . Hence in diffusing flow the net shear force on a particle of fluid of velocity greater than U_0 must be negative, as its total head is decreasing, and the local profile curvature will be concave downwards, i.e. concave towards U_0 . (This is assuming that the mixing length is either constant, or that it does not vary sufficiently for the differential of shear force to be of different sign from the second differential of velocity; it therefore excludes any region very close to a wall.) Similarly the net shear force on a particle of fluid of velocity less than U_0 , but still positive, will be positive, the velocity profile being concave upwards and towards U_0 . Thus the velocity profile in diffusing flow must be an oscillatory function of ϕ oscillating about the value of $U = U_0$. (This is consistent with the root mean square result of the previous Section 5.4.1.)

In accelerating flow the net shear force on a particle of velocity greater than U_0 must be positive and the profile concave upwards and away from U_0 . Hence the profile cannot be an oscillatory function of ϕ but the velocity must increase continuously, to infinity, or to a boundary, on either side of a position of minimum velocity. For a particle of velocity less than U_0 , but still positive, the net shear force must be negative and the profile concave downwards and away from U_0 . Hence the velocity still cannot be a (positive) oscillatory function of ϕ but must decrease at least to zero, or to a boundary, on either side of a position of maximum velocity.

Thus, while diffusing flows have velocity profiles which are oscillatory functions of ϕ , oscillating about the value U_0 , as in Figure 7a, accelerating flows have velocity profiles which cannot oscillate if entirely positive, but must consist either of a semi-infinite loop entirely above U_0 , or a loop going to zero, or to a boundary, entirely below U_0 , as in Figure 7b.

Diffusing and accelerating flows combine when the amplitude of the oscillation in diffusing flow is such that the velocity locally becomes negative, and therefore accelerating, or when the arms of the lower loop of the accelerating flow are continued to become negative, and therefore diffusing. In the latter flow the negative velocity, now a diffusing flow, will continue negative until it exceeds U_0 , as only when it exceeds U_0 may it reach a numerical maximum (as argued for diffusing flows above). After the maximum the profile velocity will then decrease, numerically. It has thus become an oscillatory function and one and the same thing as the oscillatory diffusing flow in which the amplitude is such that the velocity has locally become negative. Such a profile is illustrated in Figure 8a. If the amplitude of this flow profile increases further until the accelerating peak velocity reaches U_0 , and tends to exceed it, the accelerating peak will "burst", since the positive accelerating flow would not be able to have a maximum above U_0 . Hence the profile will consist of a semi-infinite loop with the peak as a diffusing velocity exceeding U_0 and the tails being infinite and accelerating, as in Figure 8b.

Thus a mixed flow profile can either be an oscillatory function of ϕ with the diffusing peak velocity exceeding U_0 and the accelerating peak velocity numerically less than U_0 (Figure 8a), or it can consist of a semi-infinite loop crossing both velocities U_0 and being infinite on the accelerating side (Figure 8b).

The above conclusions may be confirmed from the simple differential equation for the free two-dimensional flow of Section 3.2. Taking diffusing velocities as positive the differential equation is

$$\frac{d}{dy} (q'^2) = \frac{\lambda}{2c^2} (1 - q^2) \dots\dots\dots (58)_{bis}$$

Putting, without linearisation,

$$q = (1 + t) \dots\dots\dots (60)_{bis}$$

the equation becomes

$$2 t' t'' = - \frac{\lambda}{2c^2} (2 t + t^2) \dots\dots\dots (101)$$

Multiplying by t' and integrating,

$$\frac{2t'^3}{3} = - \frac{\lambda}{2c^2} \left(t^2 + \frac{t^3}{3} \right) + \text{constant} \dots\dots\dots (102)$$

Therefore points of maximum and minimum velocity satisfy the cubic equation:

$$f(t) = t^3 + 3t^2 + a = 0 \quad \dots\dots\dots(103)$$

Since

$$f'(t) = 3t^2 + 6t \quad \dots\dots\dots(104)$$

$f'(t) = 0$	either	when	$t = 0$	}	(See Figure 9)
		or	$t = -2$		
also $f(t) = a$		when	$t = 0$		
and $f(t) = 4 + a$		when	$t = -2$		
while $f \rightarrow -\infty$		when	$t \rightarrow -\infty$		
and $f \rightarrow +\infty$		when	$t \rightarrow +\infty$		$\dots\dots\dots(105)$

The equation is simplest when $a = 0$. There is then a double root at $t = 0$, i.e. at $u_r = U_0$. This corresponds to a diffusing flow of uniform velocity, and it also represents the limit of the oscillatory profile where the amplitude of the oscillation has become zero. The large negative root, when $a = 0$, corresponds to the peak of a semi-infinite accelerating loop. The remainder of the characteristics mentioned above may readily be obtained by tracing the behaviour of the roots of the equation from Figure 9 as the parameter 'a' is varied. The two larger roots, when real, must represent the peaks of an oscillatory profile (by an argument of 'continuity' from $a = 0$); a value for $t > -1$ corresponds to $u_r > 0$ and therefore to locally diffusing radial flow, while $t < -1$ corresponds to $u_r < 0$ and to locally accelerating radial flow.

6.0 Conclusions

(1) Exact solutions of the equation of motion are possible for various types of diffuser. Application is restricted to that part of each diffuser in which the velocity profile has attained a constant shape.

(2) It is possible to predict the critical angle of a diffuser for just avoiding flow separation provided the mixing length distribution is known; the value of the critical angle is proportional to the square of the mixing length.

(3) It is deduced that the circular cone diffuser just at separation has a turbulence level at least 30 per cent higher than that of flow in a parallel pipe. Flows having more rapid diffusion than the simple circular cone would be expected to reach an even higher turbulence level, while slower diffusion would correspondingly give a smaller increase in turbulence. The maximum value of $\frac{(u'_r u'_\theta)^2}{U_0}$ for the circular cone diffuser at separation is at least 20 per cent.

(4) If the mixing length close to the wall increases linearly with the distance from the wall, the velocity profile in the separation condition approaches the form $u_r \propto y^2$.

(5) The solutions suggest that, as an alternative to side jets, a central wake may be used for increasing the maximum rate of diffusion. For a two-dimensional diffuser a total angle considerably in excess of 30° should be attainable by either means without flow separation - provided precautions can be taken at the diffuser entry.

(6) For a side jet to persist a long distance downstream its velocity at any axial station must exceed twice the mean velocity at that station. The relative power required for the jet is high, being about 40 per cent of the power in the main part of the flow - this applies to a diffuser which has a fully developed profile at entry. If the diffuser is short so that persistence of the jet is not so important the power required for the jet should be much less.

(7) Even in a flow which is diffusing rapidly a narrow wake would be attenuated by its own turbulence. Similarly a large central wake, as from the bullet of a fan or turbine, is attenuated if the flow is of moderate diffusion angle. However, as mentioned in (5) above, a central wake, especially if produced by a high turbulence grid, could probably be used to advantage - for preventing flow separation in diffusers of very large angle.

(8) A two-dimensional radial flow with "free turbulence" has certain limitations on the shape of its velocity profile. As an example the profile cannot be periodic if the maximum diffusing velocity exceeds $2U_0$, where U_0 is defined by $p + \frac{1}{2}\rho U_0^2 = \text{const.}$

(9) Although the simple form for the turbulent shear stress as conventionally assumed in mixing length theory, i.e. $\tau = \rho L^2 \left(\frac{\partial u}{\partial Y} \right)^2$, is not consistent on transformation of axes, the errors compared with a more general form are small. In principle the latter form still permits solutions of the equations of motion, but the solutions using the simpler form are much more tractable.

LIST OF SYMBOLS

- $2c$ = diffuser total angle
- $2h$ = diffuser total width along an arc, or section diameter along an arc for the axi-symmetric diffuser
- y' = distance along an arc either from the wall or from the minimum point on a velocity profile
- y = y'/h , or y'/b
- X, Y = cartesian co-ordinates
- r, ϕ = polar co-ordinates; r = distance from diffuser vertex or from centre of radial flow
- L = mixing length
- ξ = $\frac{L}{r}$
- K = $\left(\frac{\partial L}{\partial y'} \right)_{y'=0}$ the value used in most of the calculations is $K = 0.100$
- f = $\frac{L}{Kh}$
- $2b$ = linear "wavelength", along an arc, of a velocity profile in free two-dimensional flow
- λ = angular wavelength ($2b = r\lambda$)
- c = $\frac{L}{b}$
- $\left. \begin{matrix} u_X, u_Y, \\ u_r, u_\phi \end{matrix} \right\}$ = velocity components in directions X, Y, r and ϕ . The component u_ϕ is zero for all the flows considered
- p = static pressure
- p_{1j} = stress in direction j on surface whose normal is in direction 1

P_{∞} = static pressure at infinity

τ = shear stress, simpler form

U_0 = the velocity such that $p + \frac{1}{2}\rho U_0^2 = P_{\infty}$

g = $r u_r$ or $r^2 u_r$, according as to whether the flow is two-dimensional or axis-symmetric

g' = differential of g with respect to the appropriate independent variable, ϕ , y' , y or η

g_0 = $r U_0$ or $r^2 U_0$, as for g

q = $g/g_0 = u_r/U_0$

t = $(q - 1)$

t_M = maximum value of t

t_m = minimum value of t , i.e. $(-t_m)$ is the maximum value of $(-t)$

δ_1 = value of y at the point of peak velocity in the jet, for the diffuser which has side jets for preventing flow separation

δ_2 = value of y at the point of minimum velocity between the jet and the main flow, for the diffuser which has side jets for preventing flow separation

δ = value of y at the point of peak velocity in the jet, for the diffuser powered by injection

η = y/δ_2

ρ = fluid density

μ = fluid viscosity

ν = fluid kinematic viscosity = μ/ρ

- J, e_{XX}
etc = Symbols defined by Equations (3) and (11) and the corresponding text
- B = constant defined by Equation (20)
- I = parameter defined by Equation (40)
- γ = function defined by Equation (73); $\gamma' = \frac{d\gamma}{d\eta}$
- ε = difference defined by Equation (78a)
- q_1, q_2 = values of q at $y = \delta_1$ and $y = \delta_2$
- q_3, q_4 = quantities defined by Equations (76) and (80)
- n = factor such that $(n h \delta_1) =$ equivalent jet width
- $\overline{u'_r u'_\phi}$ = mean value of the product $u'_r u'_\phi$ where u'_r is the eddy velocity in direction i
- A = cross sectional area of the flow
- g_M = maximum value of g
- g_m = minimum value of g
- $G = \frac{g_M - g_m}{g_M + g_m}$

REFERENCES

<u>No.</u>	<u>Author(s)</u>	<u>Title etc.</u>	
1	G. A. Gourzhienko (Translation)	"Formulae for velocity profiles and pressure distributions for turbulent diffusers of small angle". N.A.C.A. TM 1137, 1939 and 1947.	
2	W. F. Durand (ed.)	Aerodynamic Theory Vol.III, Section 25, p.162. (The momentum transfer hypothesis). Edited from California. 1943 edition. See also Reference 7 but pp. 206 to 8.	
3	F. Dönch	Forschungsarbeiten des Ver. deutsch. Ing. No. 282, 1926, p. 57.	
4	J. Nikuradse	Forschungsarbeiten des Ver. deutsch. Ing. No. 289, 1929, p. 42.	
5	H. Ludweig and W. Tillmann	"Investigations of the wall shearing stress in turbulent boundary layers". N.A.C.A. TM. 1285 (translation 1950).	
6	H. B. Squire	"Experiments on conical diffusers". R & M No. 2751, November, 1950.	
7	S. Goldstein (ed.)	Modern developments in fluid dynamics. Vol.I, Chapter 5, p.208. (The generalised version by Prandtl). Oxford University Press, 1938.	
8.	S. Goldstein (ed.)	Modern developments in fluid dynamics. Vol.I, Chapter 5, p. 208. (The generalised version by Prandtl). Oxford University Press, 1938.	
{	9.	B. S. Stratford	The turbulent boundary layer at separation. N.G.T.E. Note NT. 238. April, 1956.
	9.		An experimental flow with zero skin friction throughout its region of pressure rise. N.G.T.E. Note NT. 245. July, 1956.
10	S. Goldstein (ed.)	As Reference 7 but Vol.II, Chapter 8, p.372. (Limiting angle for two-dimensional diffuser).	
11	S. Goldstein (ed.)	As Reference 7 but Vol.II, Chapter 13, pp. 586 to 8. (The turbulent wake behind a row of parallel rods).	
12	H. Hagedorn and P. Ruden	Windkanaluntersuchungen an einem Junkers- Doppelflügel mit Ausblaseschlitz am Heck des Hauptflügels. Report by the Institut für Aeromechanik und Flugtechnik der Technischen Hochschule Hannover, Lilienthal Gesellschaft Bericht A.64, 1938. Also available as the R.A.E. Library Transla- tion No. 442, 1955.	

REFERENCES (Cont'd)

<u>No.</u>	<u>Author(s)</u>	<u>Title, etc.</u>
13	Ph. Poisson-Quinton	"Theoretical and experimental researches on boundary-layer control." Proc. Seventh Int. Congr. Appl. Mech. Vol.2, Part II, 1948.
14	B. S. Stratford	Unpublished work on boundary layer control by injection from aircraft gas turbine engines. N.G.T.R., July, 1953.

APPENDIX I

A tentative estimate of the effect of linearisation on the results for two-dimensional radial flow with free turbulence

The derivation without linearisation results in the Equation (102) of Section 5.4.2,

$$\frac{2t'^3}{3} = -\frac{\lambda}{2c^2} \left(t^2 + \frac{t^3}{3} \right) + \text{const.} \dots\dots\dots (102)_{\text{bis}}$$

i.e.,

$$\frac{dt}{dy} = \left[-\frac{3\lambda}{4c^2} \left(t^2 + \frac{t^3}{3} \right) + \text{const.} \right]^{\frac{1}{3}}$$

$$t = t_{\text{max.}}$$

$$\int_{t = t_{\text{min.}}}^{t = t_{\text{max.}}} \frac{dt}{\left[\text{const.} - \left(t^2 + \frac{t^3}{3} \right) \right]^{\frac{1}{3}}} = \left(\frac{3\lambda}{4c^2} \right)^{\frac{1}{3}} \left[y \right]_0^1$$

and therefore

$$\lambda = \frac{4c^2}{3} \left\{ \int_{t = t_{\text{min.}}}^{t = t_{\text{max.}}} \frac{dt}{\left[\text{const.} - \left(t^2 + \frac{t^3}{3} \right) \right]^{\frac{1}{3}}} \right\}^3 \dots\dots\dots (106)$$

The value of the constant in Equation (106) is such that the denominator becomes zero at the maximum and minimum values of 't', as shown by Equation (102) and the subsequent discussion of Section 5.4.2.

When the equation is linearised the $\frac{t^3}{3}$ term is omitted from the denominator of Equation (106). Some tentative results for the non-linearised theory suggested by a laboured estimate of the effects of the $\frac{t^3}{3}$ term are as follows. The results are given in terms of the function 'g' defined by

$$u_r = \frac{\sigma}{r} \dots\dots\dots (9)_{\text{bis}}$$

Let the maximum and minimum values of g be g_M and g_m respectively. Defining 'G' by

$$G = \frac{g_M - g_m}{g_M + g_m} \dots\dots\dots(107)$$

the value suggested for the angular wavelength of the velocity profile is

$$\lambda \doteq 23.1 \left(\frac{L}{b} \right)^2 G (1 + 0.12 G^2)$$

while the root mean square value of g , i.e. g_o , which defines the pressure rise, may be found as

$$g_o \doteq \frac{g_M + g_m}{2} (1 + 0.17 G^2)$$

The maximum and minimum values of t , i.e., the values defined by

$$t_M = (q_{max.} - 1) = \frac{g_M - g_o}{g_o}$$

and

$$t_m = -(1 - q_{min.}) = -\frac{g_o - g_{min.}}{g_o}$$

become

$$t_M \doteq G \left(1 - \frac{G}{6} - \frac{G^2}{6} \right)$$

$$t_m \doteq -G \left(1 + \frac{G}{6} - \frac{G^2}{6} \right)$$

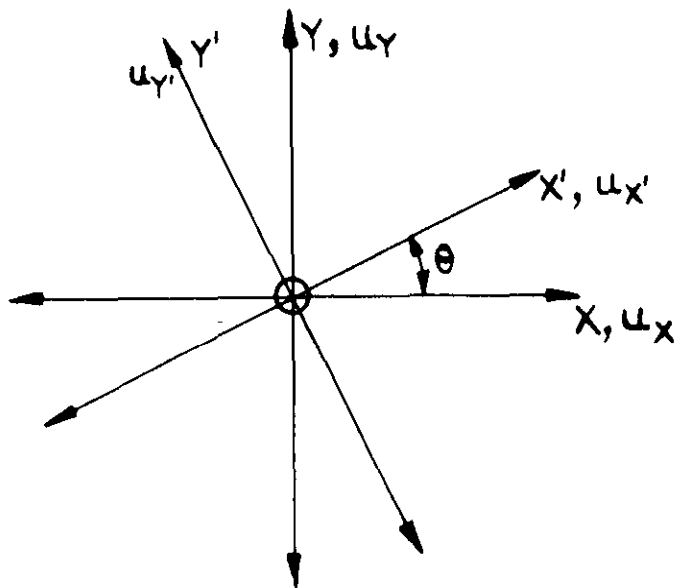
The angular wavelength in terms of say $(-t_m)$ is suggested as

$$\lambda \doteq \frac{23.1 \left(\frac{L}{b} \right)^2 \cdot (-t_m)}{\left[1 + 0.17 (-t_m) - 0.32 (-t_m)^2 \right]}$$

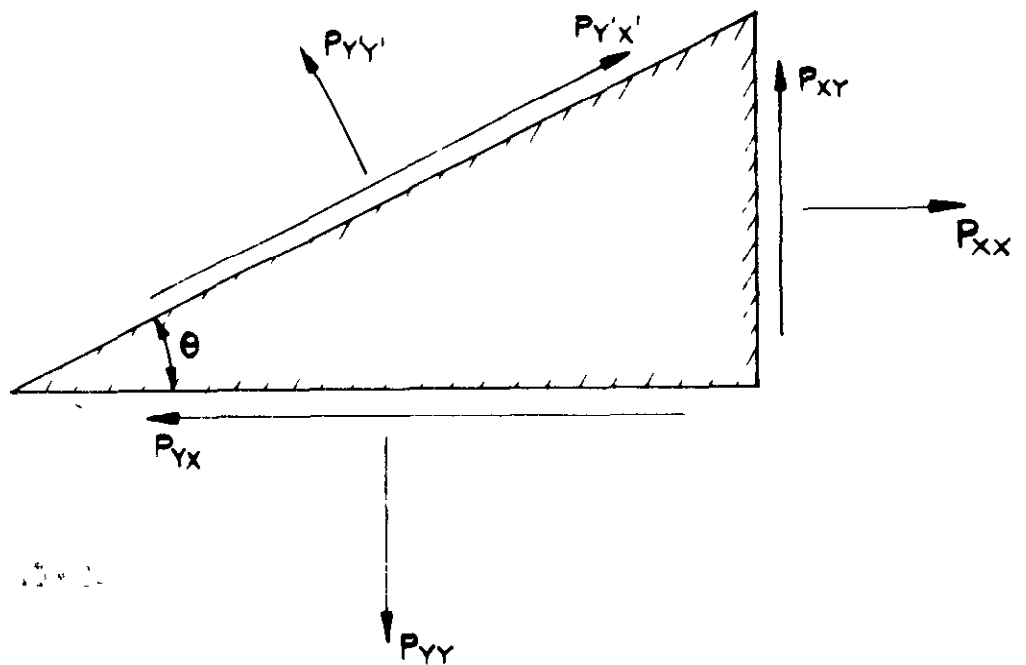




FIG. 1

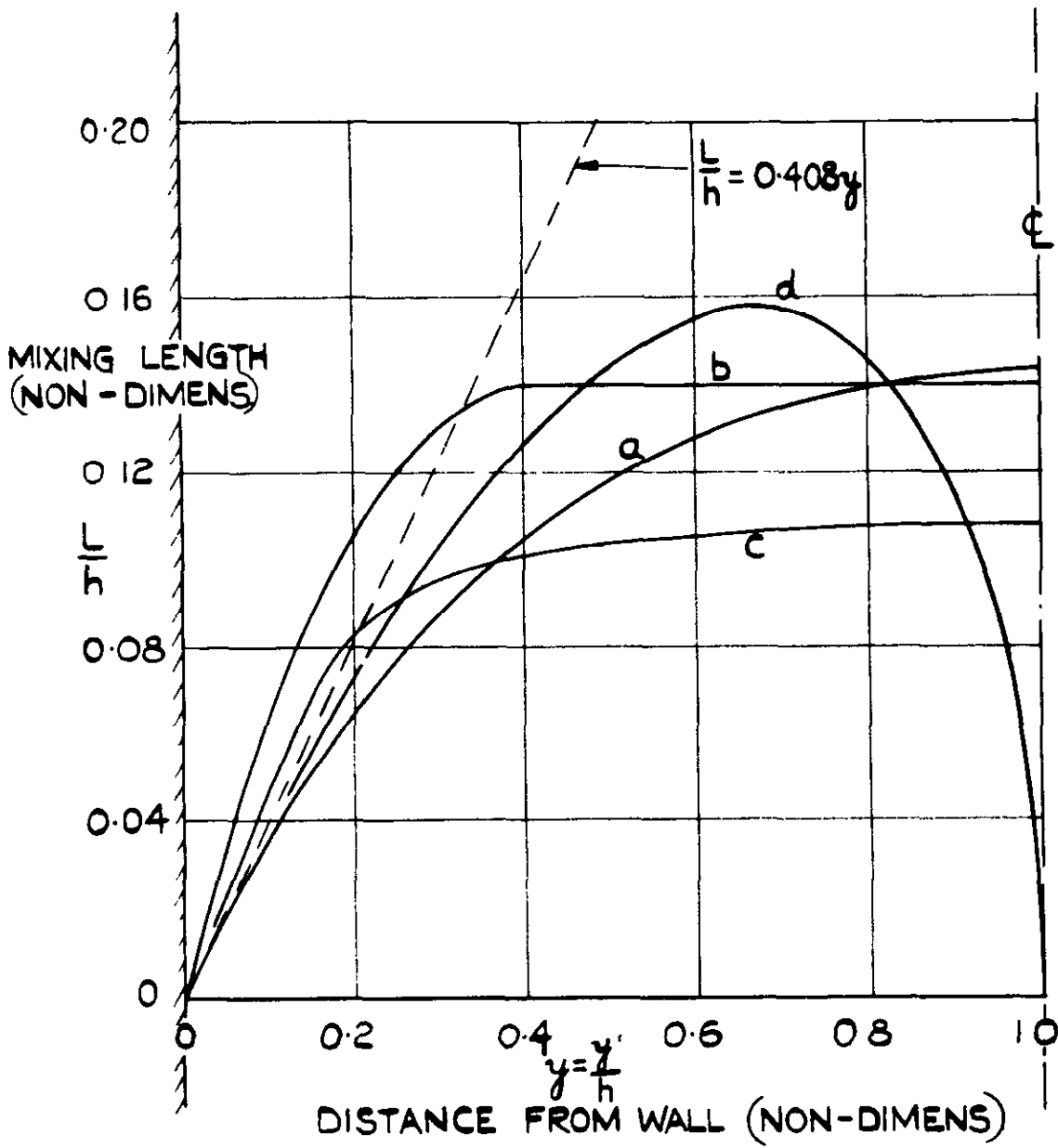


[CHANGE OF AXES FROM X, Y TO X', Y']



THE STRESSES ON A SMALL WEDGE OF FLUID

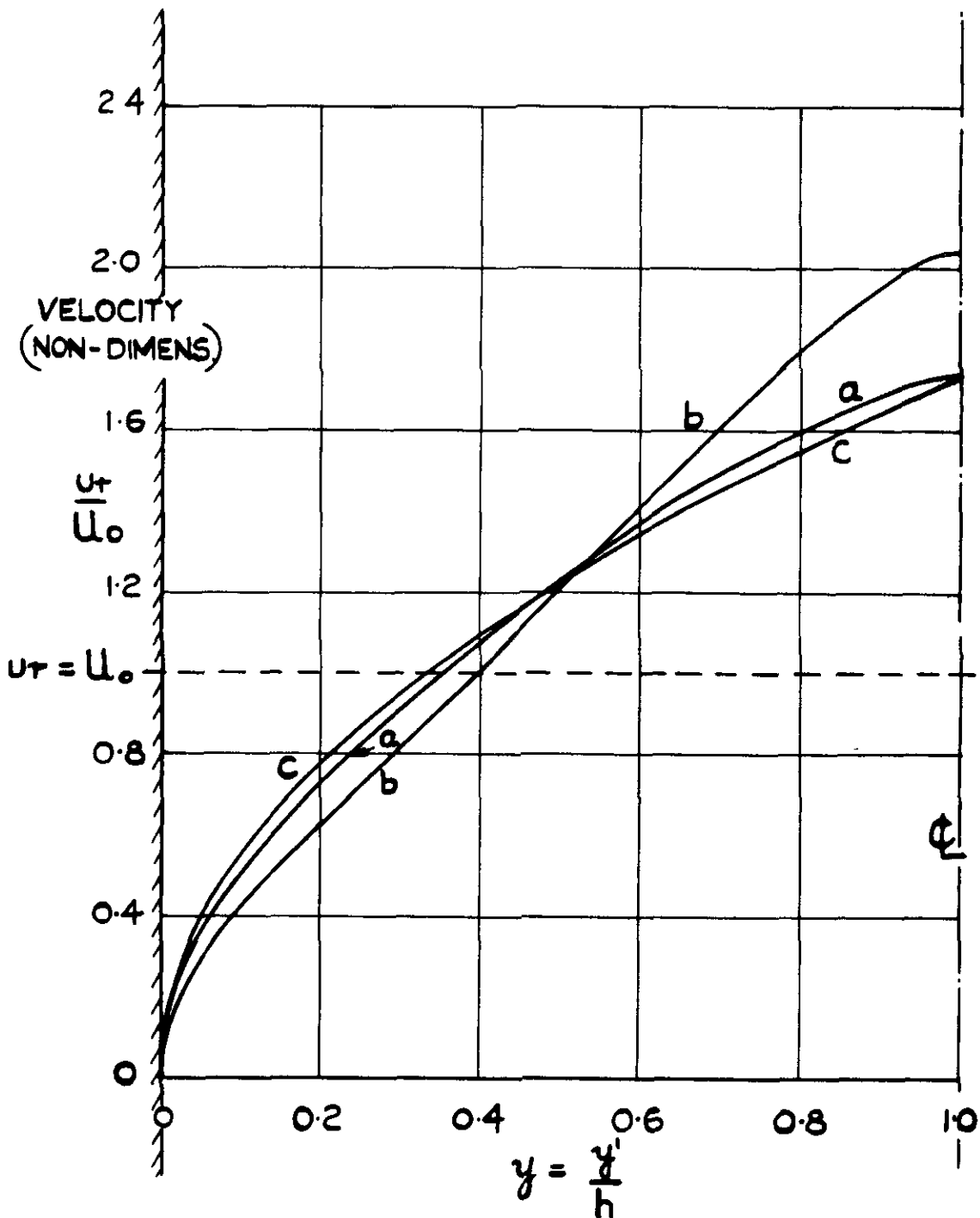
FIG. 2



- KEY CURVE a, UNIVERSAL MIXING LENGTH DISTRIBUTION L_0
 CURVE b; L_{DN} =DISTRIBUTION ACCORDING TO DONCH & NIKURADSE
 CURVE c, L_1
 CURVE d; $L_s = 0.408hy (1-y)^{\frac{1}{2}}$
 $h =$ DIFFUSER SEMI-WIDTH OR SEMI-DIAMETER

VARIOUS MIXING LENGTH DISTRIBUTIONS

FIG. 3



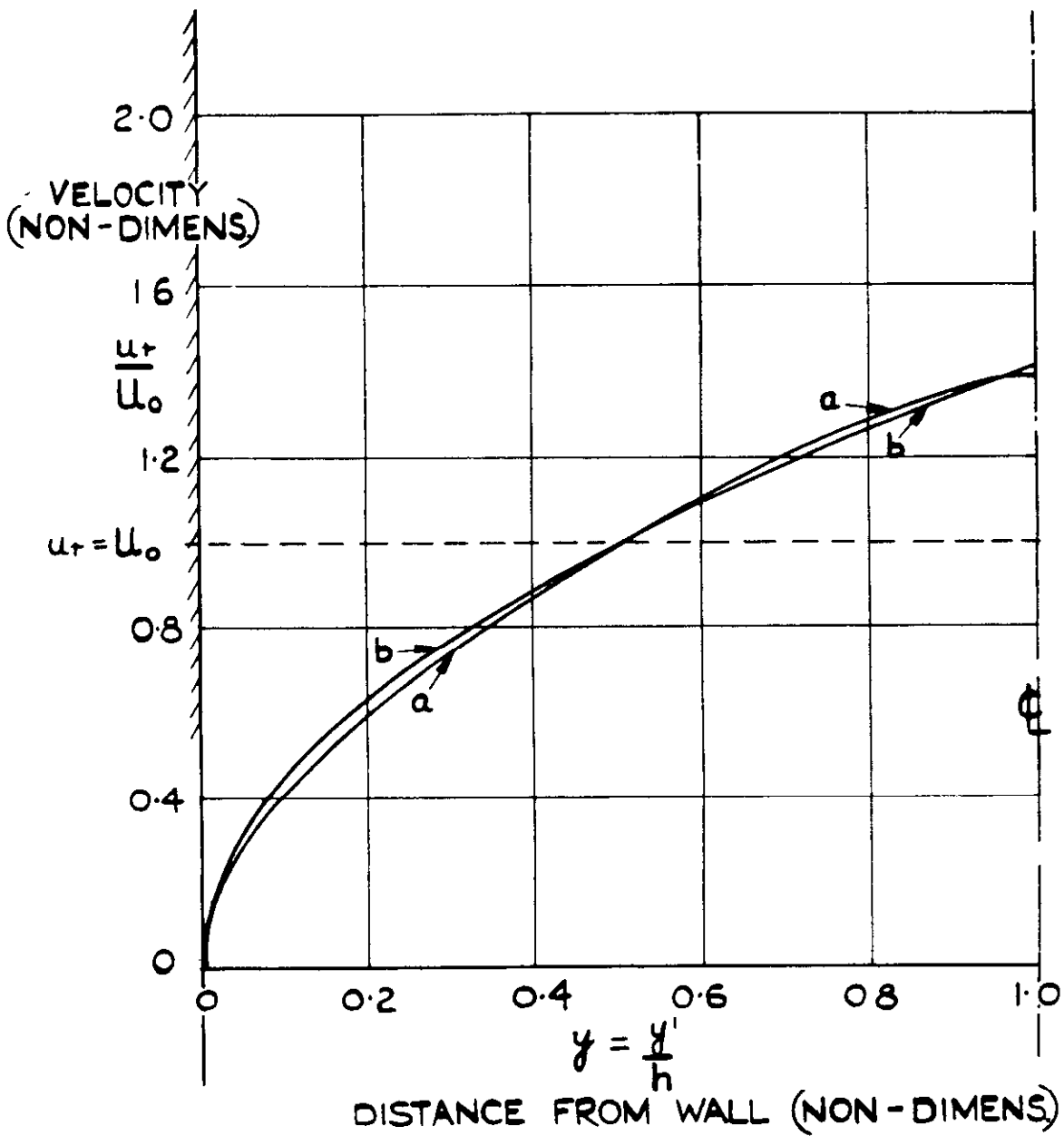
DISTANCE FROM WALL (NON-DIMENS)

- KEY
- CURVE 'a'; PROFILE DERIVED FROM L_0 ($2\alpha = 6.08^\circ$)
 - CURVE 'b'; PROFILE DERIVED FROM L_{DN} ($2\alpha = 13.3^\circ$)
 - CURVE 'c'; PROFILE DERIVED FROM L_s ($2\alpha = 7.15^\circ$)

PROFILE 'c' IS $\frac{u_r}{u_0} = (3y)^{\frac{1}{2}}$

VARIOUS VELOCITY PROFILES FOR THE AXI-SYMMETRIC DIFFUSER AT SEPARATION

FIG. 4



KEY CURVE a; PROFILE DERIVED FROM L_0
 CURVE b; PROFILE DERIVED FROM L_s
 PROFILE 'b' IS $\frac{u_r}{u_0} = (2y)^{\frac{1}{2}}$

VARIOUS VELOCITY PROFILES FOR THE TWO-DIMENSIONAL DIFFUSER AT SEPARATION

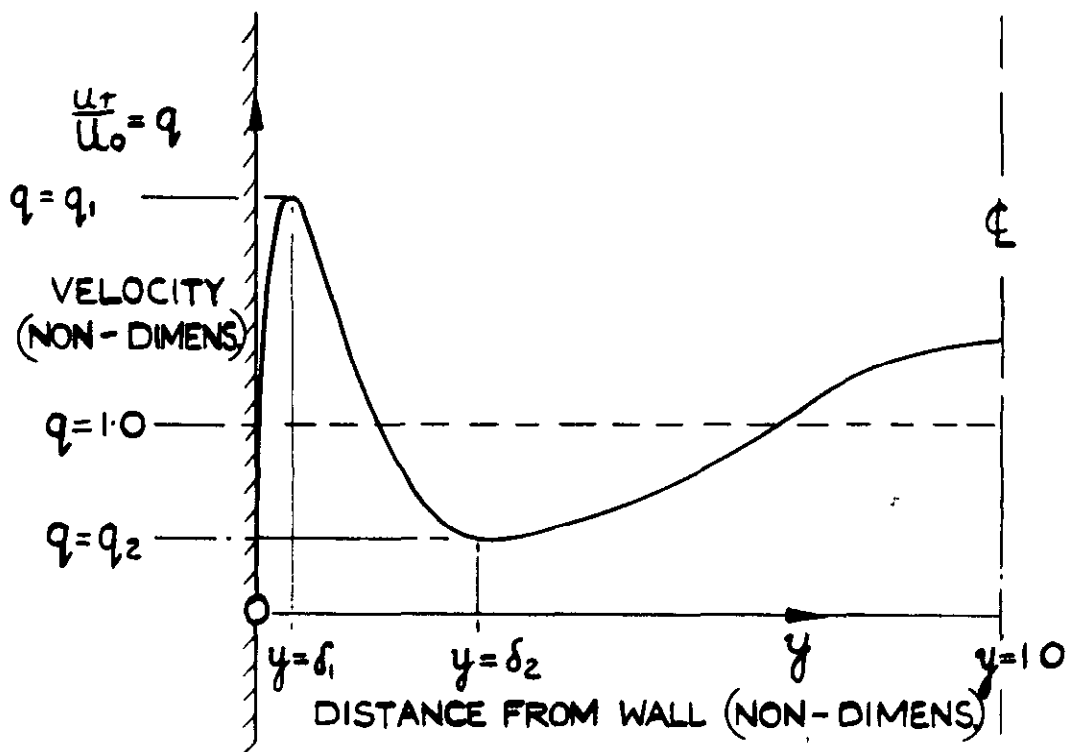


FIG. 5a A DIFFUSER WITH CONTROL BY SIDE JETS

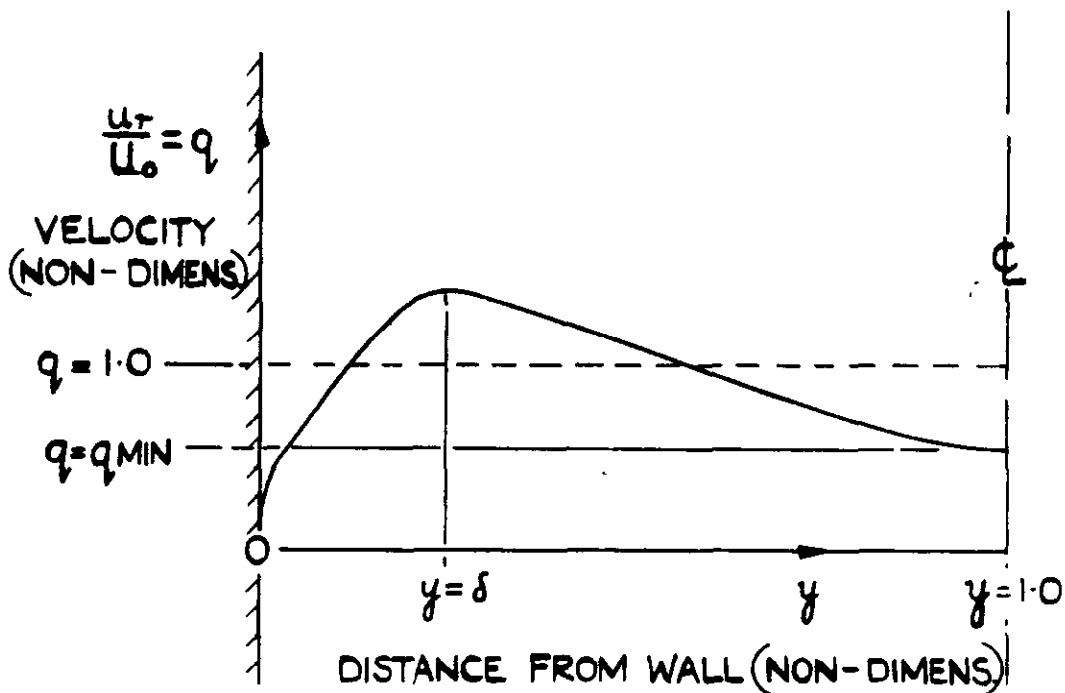
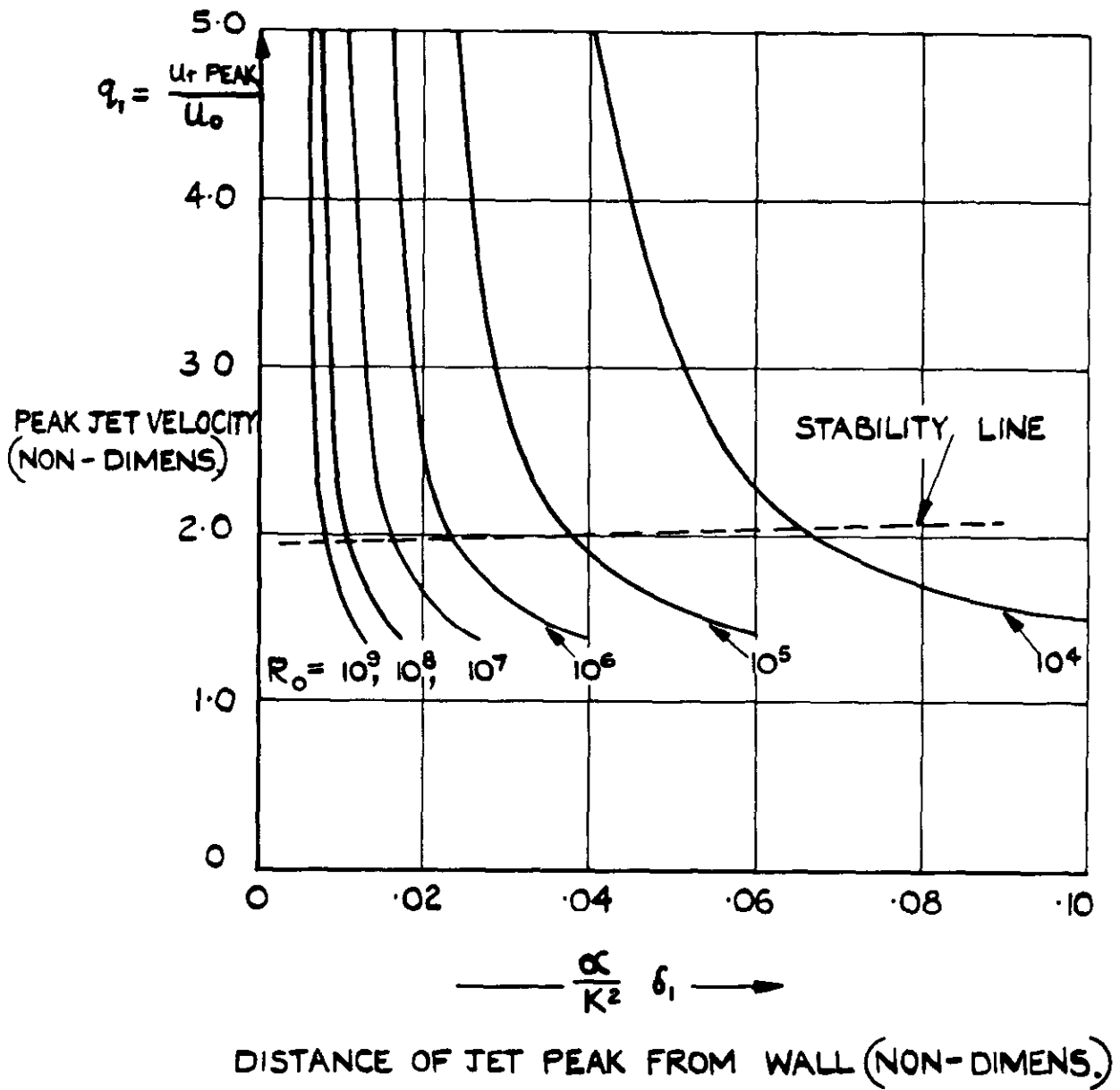


FIG. 5b DIFFUSER OF A WIND TUNNEL POWERED BY INJECTION, OR, DIFFUSER WITH A CENTRAL WAKE.

TYPES OF VELOCITY PROFILES FOR DIFFUSERS WITH SIDE JETS OR A CENTRAL WAKE.

FIG. 6



$$R_o = \frac{h U_0}{\nu}$$

THE SOLUTION FOR THE 'BOUNDARY LAYER' OF THE JET.

FIG.7

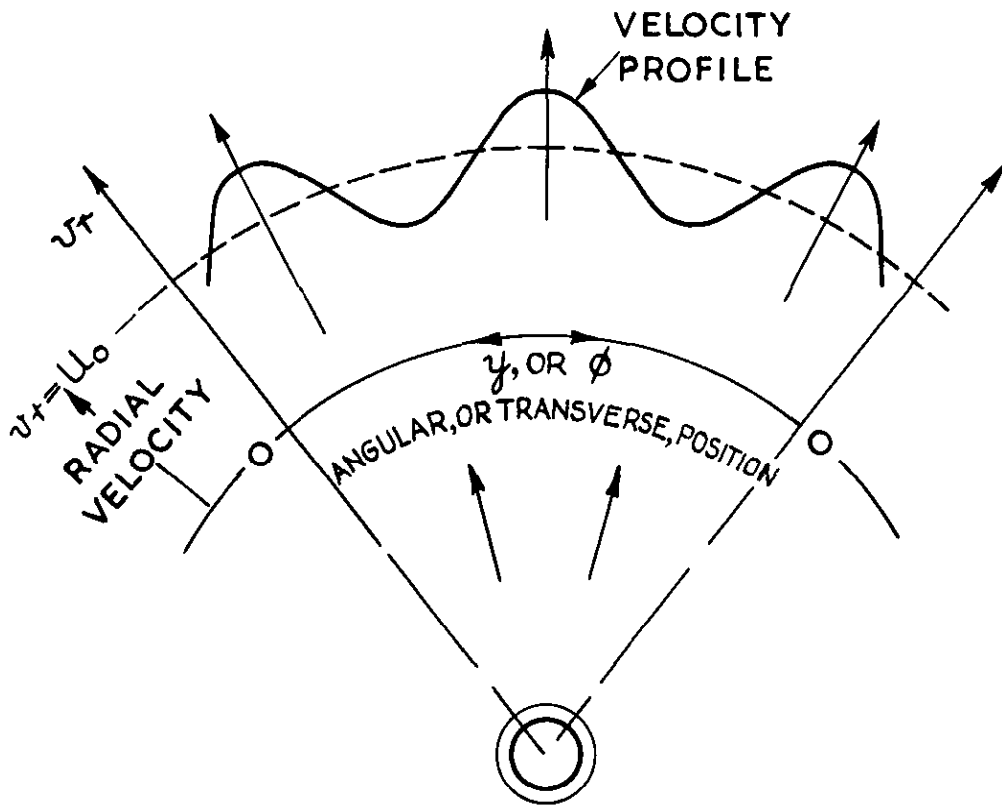


FIG.7a. DIFFUSING RADIAL FLOW

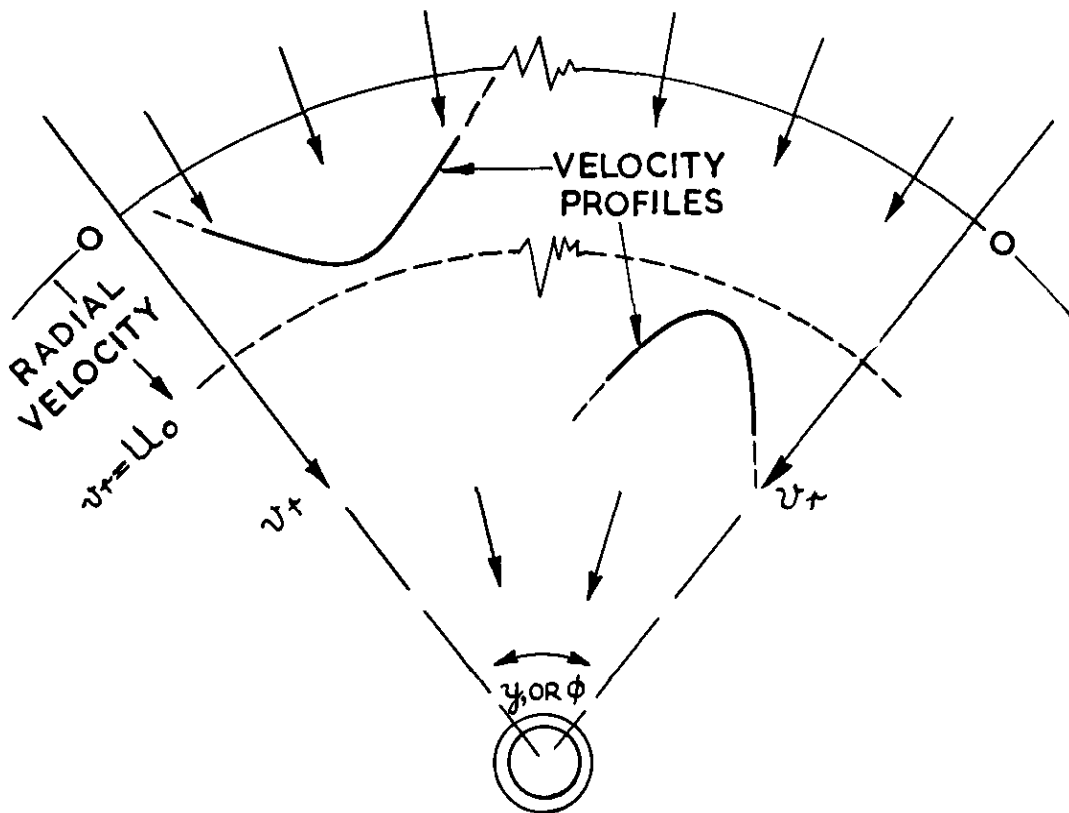


FIG.7b. ACCELERATING RADIAL FLOW

TYPES OF VELOCITY PROFILES IN FREE
TWO-DIMENSIONAL FLOW DIFFUSING FLOW
& ACCELERATING FLOW

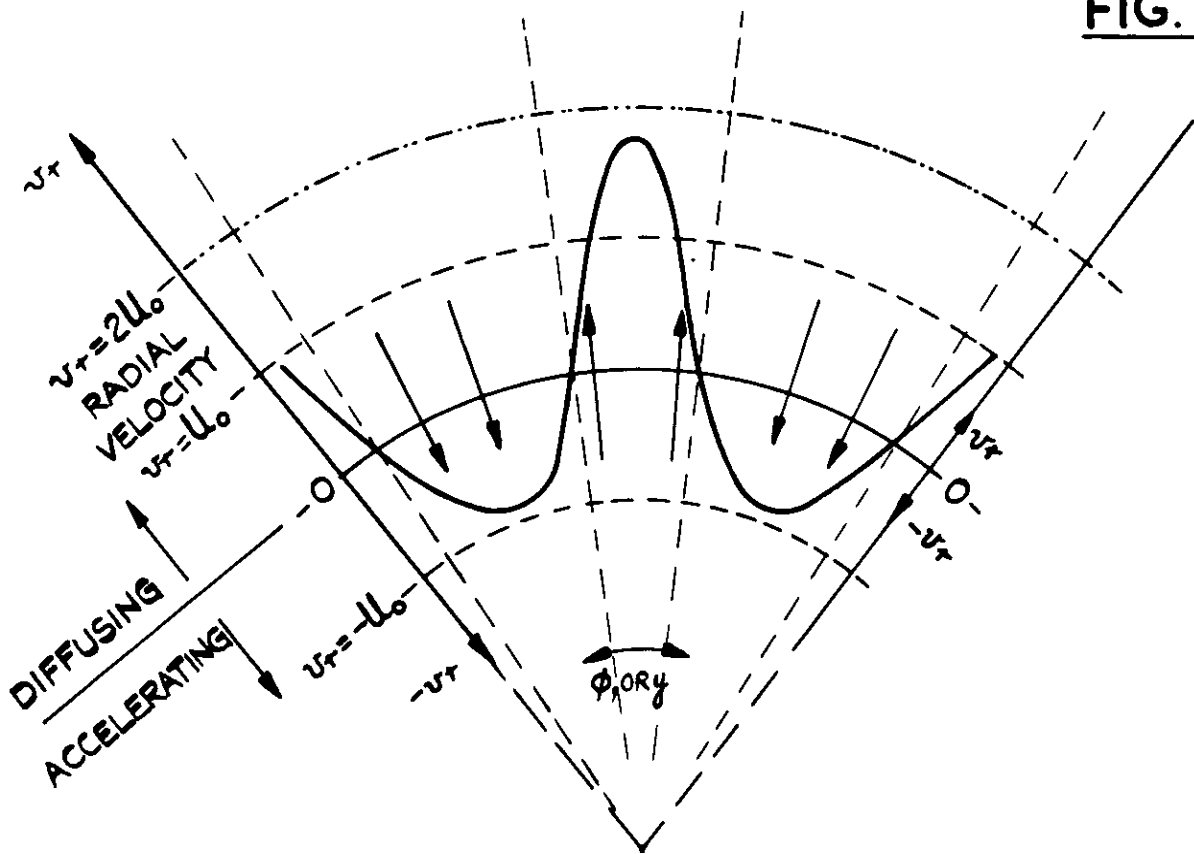


FIG. 8a PROFILE PERIODIC.

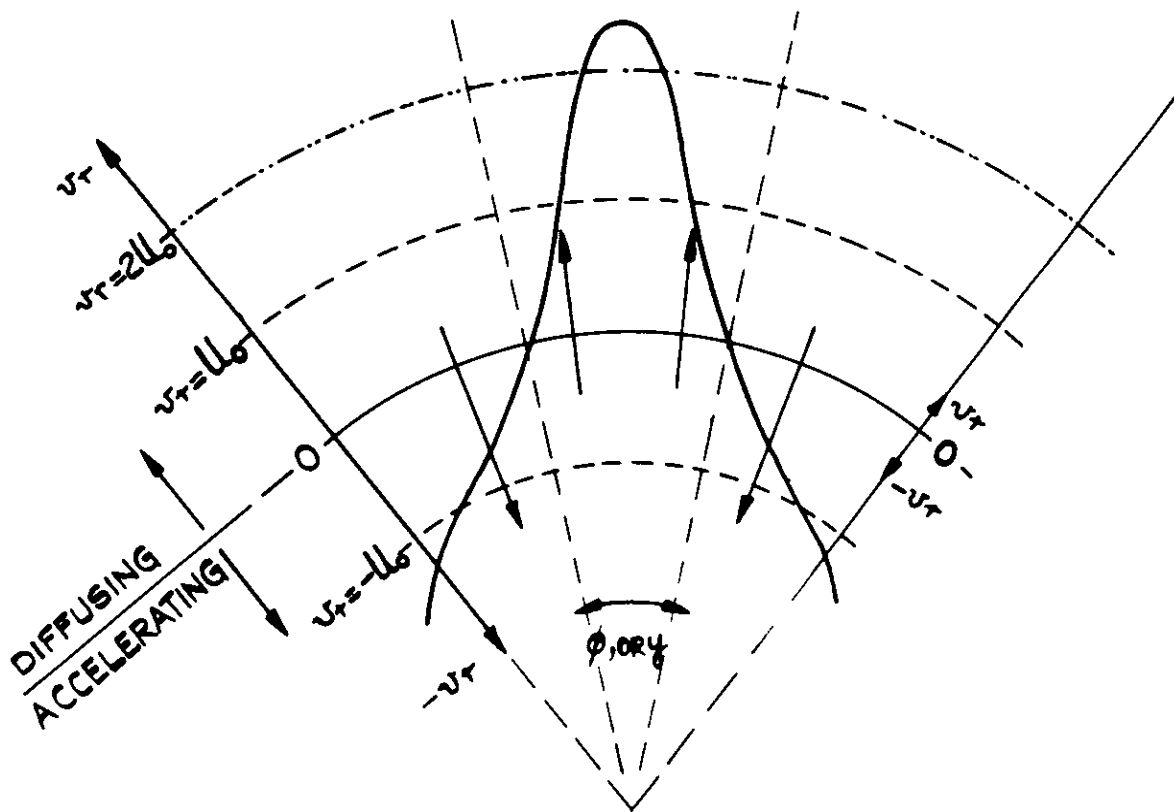
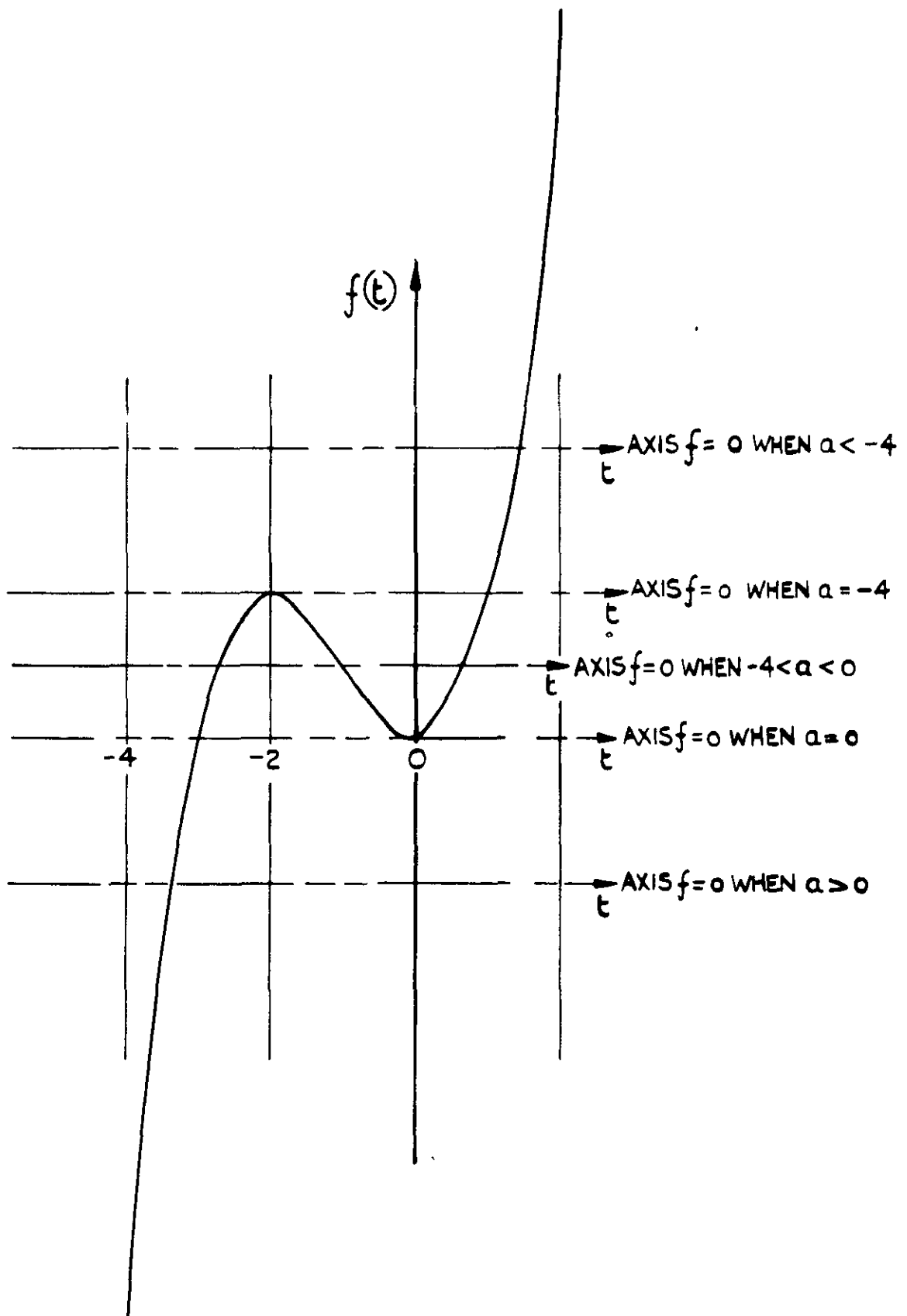


FIG. 8b PROFILE NON-PERIODIC

TYPES OF VELOCITY PROFILE IN FREE
TWO-DIMENSIONAL FLOW, MIXED
DIFFUSING & ACCELERATING FLOW.

FIG. 9



THE CUBIC EQUATION FOR FREE
TWO-DIMENSIONAL RADIAL FLOW.



Crown copyright reserved

Printed and published by
HER MAJESTY'S STATIONERY OFFICE

To be purchased from
York House, Kingsway, London W.C.2
423 Oxford Street, London W.1
P.O. Box 569, London S.E.1
13A Castle Street, Edinburgh 2
109 St. Mary Street, Cardiff
39 King Street, Manchester 2
Tower Lane, Bristol 1
2 Edmund Street, Birmingham 3
80 Chichester Street, Belfast
or through any bookseller

Printed in Great Britain